

## Determination of the Anisotropy of the Energy Gap in Superconducting Pb by Superconductive Tunneling\*†

G. I. ROCHLIN‡

*Department of Physics and Institute for the Study of Metals, University of Chicago, Chicago, Illinois*

(Received 27 June 1966)

The anisotropy of the energy gap in superconducting Pb has been studied experimentally by the method of superconductive tunneling. Structure due to the Pb anisotropy has been observed in thick-Pb-versus-Al tunneling junctions at biases equal to the sum of the gaps. The theory has been analyzed and the experimental line shapes have been compared with theoretical predictions. Structure arising from the energy-gap anisotropy has also been observed in the subharmonic structure—below  $2\Delta$ —in Pb-versus-Pb tunneling junctions. These data have been interpreted in terms of the critical values—maxima, minima, and saddle points—of the energy-gap surface in  $k$  space. The double energy gap  $2\Delta$  has been observed to have a maximum at  $2.98 \pm 0.03$  meV and saddle points at  $2.44 \pm 0.02$  and  $2.55 \pm 0.02$  meV. Additional structure has been observed in the subharmonic region which yields leading terms in the subharmonic series at  $2.11 \pm 0.02$ ,  $2.23 \pm 0.02$ ,  $2.33 \pm 0.02$ ,  $2.39 \pm 0.02$ , and  $2.61 \pm 0.02$  meV. These latter values represent either critical values of the gap or the average of two such critical values. The present status of the theory of the subharmonic structure is discussed briefly.

### I. INTRODUCTION

THERE has been considerable interest recently in the anisotropy of the superconducting energy gap, i.e., the variation of the gap with crystallographic direction. In the BCS<sup>1</sup> theory the energy gap is isotropic in  $k$  space. This is a consequence of the initial assumption of isotropic parameters in the energy-gap equation. Nevertheless, many experiments have demonstrated that the energy gap is, in fact, anisotropic in many superconducting metals.

Various attempts<sup>2,3</sup> have been made to calculate the energy-gap anisotropy under the assumption that the significant parameter was the anisotropy of the electron distribution, i.e., the band-structure effects or Fermi-surface anisotropy. However, Bennett<sup>4</sup> has recently proposed that the primary source of gap anisotropy is the anisotropy of the phonon spectrum, which enters the gap equation through the electron-phonon interaction. He has performed a calculation of the energy-gap anisotropy in Pb, a superconductor whose strong coupling nature is well known,<sup>5,6</sup> and whose band structure<sup>7,8</sup> and phonon spectrum<sup>9</sup> have been studied in

detail. In addition he has discussed several aspects of the experimental manifestations of the anisotropy.

Although many studies of energy-gap anisotropy have been made by ultrasonic attenuation<sup>10-13</sup> and electromagnetic absorption,<sup>14-16</sup> perhaps the most direct and accurate measurements of this anisotropy can be made by the method of superconductive tunneling.<sup>17-23</sup> We have performed a series of experiments to determine the anisotropy of the energy gap in superconducting Pb by means of superconductive tunneling junctions of various configurations. A large number of distinct energy gaps have been resolved in the tunneling characteristics of these junctions, one or both of whose elements consist of thick Pb films.

Structure due to anisotropy has appeared in two distinct portions of the  $I$ - $V$  characteristics of the junctions, arising from two quite different mechanisms which we have placed in two separate categories. That portion of the structure which may be described by an application of the usual theory of single-particle superconduct-

<sup>10</sup> R. W. Morse, T. Olsen, and J. D. Gavenda, *Phys. Rev. Letters* **3**, 15 (1959); **3**, 193(E) (1959).

<sup>11</sup> H. V. Bohm and N. H. Horowitz, in *Proceedings of the Eighth International Conference on Low Temperature Physics* (Butterworths Scientific Publications, Inc., Washington, 1963).

<sup>12</sup> J. R. Leibowitz, *Phys. Rev.* **133**, A84 (1964).

<sup>13</sup> L. T. Clairborne and N. G. Einspruch, *Phys. Rev. Letters* **15**, 862 (1965).

<sup>14</sup> P. L. Richards, *Phys. Rev. Letters* **7**, 412 (1961).

<sup>15</sup> M. A. Biondi, M. P. Garfunkel, and W. A. Thompson, *Phys. Rev.* **136**, A1471 (1964).

<sup>16</sup> M. A. Biondi, M. P. Garfunkel, and W. A. Thompson, in *Proceedings of the Ninth International Conference on Low Temperature Physics* (Plenum Press, Inc., New York, 1965).

<sup>17</sup> G. I. Rochlin and D. H. Douglass, Jr., *Bull. Am. Phys. Soc.* **10**, 46 (1965).

<sup>18</sup> G. I. Rochlin and D. H. Douglass, Jr., *Phys. Rev. Letters* **16**, 359 (1966).

<sup>19</sup> P. Townsend and J. Sutton, *Phys. Rev.* **128**, 591 (1962).

<sup>20</sup> N. V. Zavaritskii, *Zh. Eksperim. i Teor. Fiz.* **41**, 831 (1961) [English transl.: *Soviet Phys.—JETP* **14**, 470 (1961)].

<sup>21</sup> N. V. Zavaritskii, *Zh. Eksperim. i Teor. Fiz.* **43**, 1123 (1962) [English transl.: *Soviet Phys.—JETP* **16**, 793 (1963)].

<sup>22</sup> N. V. Zavaritskii, *Zh. Eksperim. i Teor. Fiz.* **48**, 837 (1965) [English transl.: *Soviet Phys.—JETP* **21**, 557 (1965)].

<sup>23</sup> W. J. Tomasch, *Phys. Rev.* **139**, A746 (1965).

\* Supported in part by the Army Research Office (Durham) and the Advanced Research Projects Agency.

† Submitted in partial fulfillment of the requirements for the degree of Doctor of Philosophy at the University of Chicago.

‡ Present address: Department of Physics, University of California, Berkeley, California.

<sup>1</sup> J. Bardeen, L. N. Cooper, and J. R. Schrieffer, *Phys. Rev.* **108**, 1175 (1957).

<sup>2</sup> V. L. Pokrovskii, *Zh. Eksperim. i Teor. Fiz.* **40**, 641 (1961) [English transl.: *Soviet Phys.—JETP* **13**, 447 (1961)].

<sup>3</sup> B. T. Geilikman and V. Z. Kresin, *Fiz. Tver. Tela.* **5**, 3549 (1963) [English transl.: *Soviet Phys.—Solid State* **5**, 2605 (1964)].

<sup>4</sup> A. J. Bennett, *Phys. Rev.* **140**, A1902 (1965).

<sup>5</sup> D. J. Scalapino, Y. Wada, and J. C. Swihart, *Phys. Rev. Letters* **14**, 102 (1965).

<sup>6</sup> J. C. Swihart, D. J. Scalapino, and Y. Wada, *Phys. Rev. Letters* **14**, 106 (1965).

<sup>7</sup> A. V. Gold, *Phil. Trans. Roy. Soc. (London)* **251**, 85 (1958).

<sup>8</sup> J. R. Anderson and A. V. Gold, *Phys. Rev.* **139**, A1459 (1963).

<sup>9</sup> B. N. Brockhouse, T. Arase, G. Caglioti, K. R. Rao, and A. D. B. Woods, *Phys. Rev.* **128**, 1099 (1962).

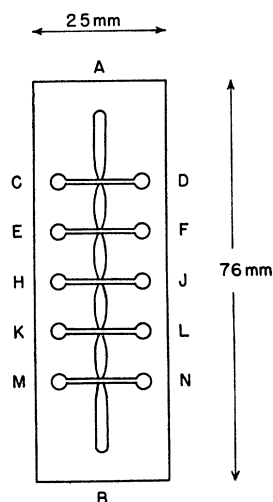


FIG. 1. Typical Pb-I-Pb sample with five junctions. The films are  $\approx 0.2$  mm wide in the junction region. A, C, E, H, K, and M are the current contacts, while B, D, F, J, L, and N are the voltage contacts.

tive tunneling has been designated as structure in the "ordinary" tunneling characteristic, and is described fully in Sec. IV. The other structure occurs in a region of bias voltage for which the ordinary tunneling current is extremely small; it has, due to its occurrence at submultiples of the gap energy, been designated "subharmonic" structure,<sup>18</sup> and is described in Sec. V.

Experimental details and sample preparation are described in Sec. II, while a brief review of Bennett's theory of the anisotropy of the energy gap of superconducting Pb is given in Sec. III. The conclusions, and a summary of our experimental results, are presented in Sec. VI, together with a discussion of the mechanisms for the subharmonic structure.

## II. EXPERIMENTAL METHODS

### A. Sample Preparation

The samples consisted of vacuum-deposited metallic-film tunneling junctions of the type Pb-I-Pb, Pb-I-Sn, Pb-I-Al, or Pb-I-Mg, where *I* designates a general insulating barrier layer 10–30 Å thick, usually obtained by thermal oxidation of one of the films. The films were deposited on standard 25-mm  $\times$  76-mm glass microscope slides by resistance heating of a refractory metal source in an ion-pumped ultra-high vacuum system<sup>24</sup> capable of base pressures below  $10^{-9}$  Torr. During evaporation of the Pb films the pressure was held below  $5 \times 10^{-8}$  Torr at all times, while pressures up to  $3 \times 10^{-7}$  Torr were tolerated during the evaporation of the other metals.

Five junctions were prepared simultaneously on a single substrate, in the geometry shown in Fig. 1, by depositing one of the metals, oxidizing it, and depositing the second metal over the oxide. The Pb was deposited as the single longitudinal strip whether it was deposited first or second. Contacts to the strips were originally made by soldering directly to the film and substrate

<sup>24</sup> Ultex Corporation Model TNB.

with Cerroseal 35, a glass-wetting tin-indium alloy solder. On later samples the contacts were made with a flexible, air drying, silver conducting paint.<sup>25</sup> Teflon-coated #40 copper wires were embedded directly in the silver-paint dots at one end, and led to a terminal strip to which the leads going out of the cryostat were attached. This terminal strip was also immersed in the liquid helium, to avoid heat leaks into the samples.

As the resistivities of the junctions vary over many orders of magnitude, depending on the metal which is oxidized, the width of the strips was varied between 0.2 mm and 1.5 mm so as to vary the area of the junctions. By this means, the total resistance of the junction was controlled in such a manner as to bring it into the region where the electrical measurements could be most conveniently made. Film thicknesses varied from 100 Å to several thousand angstroms, depending on the metal deposited and the conditions desired. After all the data was taken on a given substrate, the entire slide was vacuum plated with about 100 Å of Al, and the film thickness determined by multiple-beam interferometry<sup>26</sup> to an accuracy of  $\pm 10\%$ .

### B. Cryogenics

The measurements were performed in a stainless-steel liquid-helium cryostat at temperatures between 4.2°K and 1°K. Below the  $\lambda$  point the temperature was stabilized by an automatically regulating ac Wheatstone bridge<sup>27</sup> which is capable of maintaining the bath temperature to within 0.05 mdeg Kelvin for several hours. The sample was mounted inside a copper shield can together with 33- $\Omega$  and 100- $\Omega$  Allen-Bradley carbon resistors and a Honeywell germanium thermometer. The calibration of the carbon resistors was periodically checked against the bath pressure and the germanium thermometer. After several months of continuous use no further recalibration of these carbon resistors was found to be necessary, despite frequently severe thermal cycling.

### C. Electronics

The junction characteristics were measured by a constant-current device capable of measuring the *I-V* characteristic, the differential resistance  $dV/dI$ , and the second derivative<sup>28</sup>  $d^2V/dI^2$  of the sample as a function of the bias voltage *V*. The circuitry is shown in Fig. 2. The constant-current method was chosen primarily because it is both simpler and more accurate for measurements of samples of low resistance than other

<sup>25</sup> Type SC13 Flexible Silver Micropaint: Micro-Circuits Company, New Buffalo, Michigan.

<sup>26</sup> S. Tolansky, *Multiple Beam Interferometry* (Oxford University Press, New York, 1948).

<sup>27</sup> C. Blake, C. E. Chase, and E. Maxwell, *Rev. Sci. Instr.* **29**, 715 (1958).

<sup>28</sup> The usual theoretical calculation is for  $d^2I/dV^2$ , which is related to our measurements by  $(d^2V/dI^2) = -(dI/dV)^{-3} \times (d^2I/dV^2)$ . The actual measured signal at the second harmonic of the driving frequency is  $V_{2\omega} \propto (d^2V/dI^2)$ .

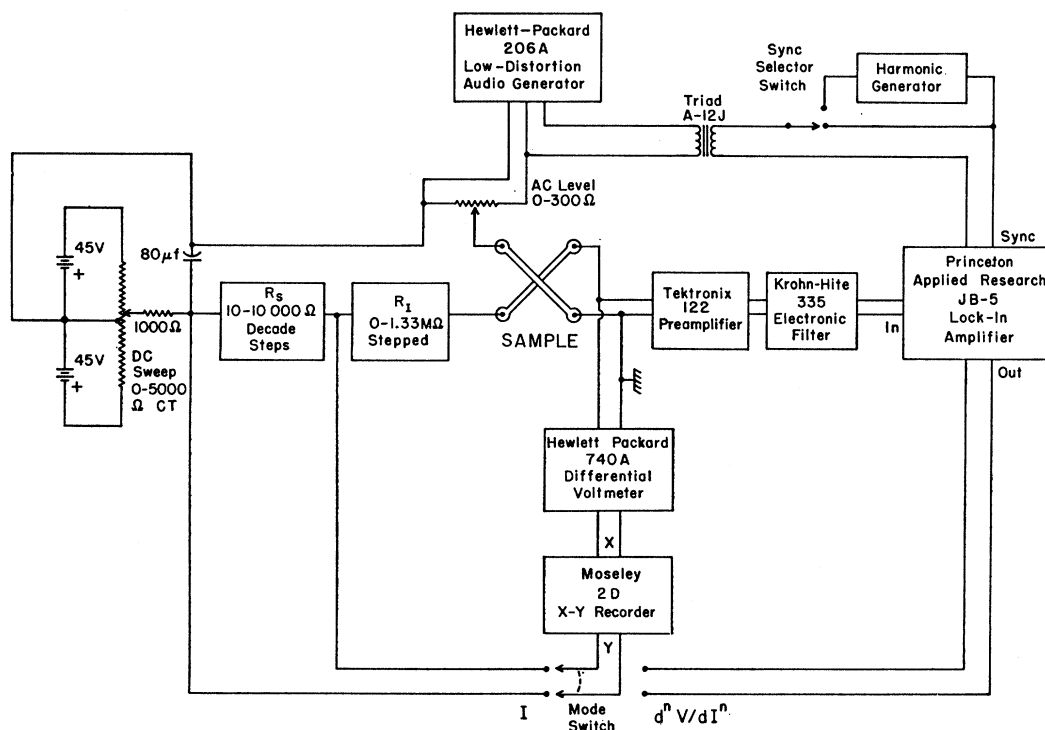


FIG. 2. Schematic of the electronics used to measure the junction characteristics.  $R_1$  is the constant-current resistor, which was set to  $\geq 1000$  times the large bias sample resistance. A small motor was used to turn the dc sweep Helipot so that the dc current was swept linearly with time. The electronic filter was used only for measuring second or higher harmonics.

methods.  $dV/dI$  measurements were made by applying a small constant ac current at a frequency of 255 Hz to the sample and measuring both the ac and dc voltages across it as the dc current was swept. Four-terminal methods were used throughout the experiment. Since the ac voltage across the junction is directly proportional to the ac resistance, the voltage resolution automatically increases in the vicinity of the  $dV/dI$  minima where the highest resolution is desired.

The applied ac current was controlled so that the voltage across the junction never exceeded  $50 \mu\text{V}$  peak-to-peak (p-p) at large dc biases (where  $dV/dI$  is nearly constant). The signal was usually  $10 \mu\text{V}$  p-p or less in the regions of maximum structure. In addition, the ac level was reduced further whenever there appeared to be structure present which was narrower in voltage than the p-p ac signal across the sample. The ac signal was amplified with a Tektronix RM 122 preamplifier, whose output was fed into a Princeton Applied Research JB-5 lock-in amplifier which was used to drive the X channel of a Moseley 2D X-Y recorder. Errors in the magnitude of  $dV/dI$  do not exceed 1%.

The dc bias was measured with a Hewlett-Packard 740A differential voltmeter, used as a 0.01% linear dc amplifier to drive the Y channel of the X-Y recorder. During every run the gain and linearity of the dc bias measuring circuit was verified by using the internal voltage reference standard and differential voltmeter modes of the dc voltmeter. Over-all linearity and ac-

curacy of the voltmeter-recorder system was better than 0.1%, being limited primarily by the linearity of the recorder.

The sample was swept continuously through zero bias without switching in order to eliminate the zero uncertainties caused by stray dc voltages and thermal emfs. The various characteristics were checked for time-lag hysteresis, which is often a problem in long time constant circuits such as this one, by reversing the direction of sweep and examining the retrace of the curves. By these means, errors in the dc bias measurements were held to less than 0.2% of the measured values of the bias. The somewhat larger errors presented in the experimental results are due to: (1) scatter in the data, and (2) the difficulty in determining the actual minimum point on some of the broader minima in  $dV/dI$ .

### III. ANISOTROPY OF THE ENERGY GAP

The early theories<sup>2,3</sup> of the anisotropy of the energy gap  $\Delta$  were based on the premise that the source of this phenomenon was to be found in the anisotropy of the electron distribution, and particularly in the effects of the Fermi surface. Under the assumption that the energy gap could not vary greatly over any single piece of the surface, it was suggested that the anisotropy reflected the various pieces of the quite complex Fermi surfaces of the various superconductors.

In particular, Zavaritskii<sup>20-22</sup> has performed a series of tunneling experiments on single crystal Sn, from which

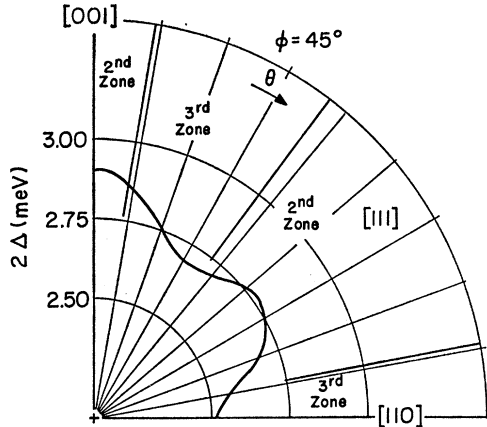


FIG. 3. The double energy gap of Pb in the (110) plane through  $\Gamma$ , in the spherical-band approximation (from Ref. 4).

he has been able to determine the variation of  $\Delta$  with crystallographic direction. This variation was plotted as areas of roughly constant  $\Delta$  on a standard crystallographic projection. The known Fermi surface of Sn was then projected onto this plot and, under the assumption that  $\Delta$  was a constant over any single piece of the Fermi surface but varied from piece to piece, an attempt was made to correlate the areas of constant  $\Delta$  with projected areas of the Fermi surface. Although the attempted fit was only partially successful, the complexity of the Fermi surface of Sn is such that this approach could not be positively ruled out.

For this reason, it is more fruitful to study the case of Pb, whose Fermi surface is accurately known and relatively simple.

The Fermi surface of Pb has recently been examined by Anderson and Gold,<sup>7,8</sup> who described the surface in terms of a four-OPW (orthogonalized-plane-wave) interpolation scheme with four adjustable parameters. The four parameters were determined by a least-squares fit to the extremal areas which they observed in their de Haas-van Alphen experiments. Their results confirmed the correctness of the nearly-free-electron surface which had been used to explain a large number of previous experiments<sup>29</sup> in which properties directly related to the Fermi surface had been measured.

Although the free-electron surface has pieces in the second, third, and fourth zones, experiment shows that the fourth zone is actually empty due to spin-orbit effects. Aside from the deviations near the zone boundaries, the surface very closely resembles a free-electron sphere in the extended-zone scheme. In the reduced-zone scheme, the surface is found to consist of only two pieces. The first of these is a multiply connected third-zone electron surface, consisting of a set of tubes along the boundaries of the first Brillouin zone. The other is a second-zone hole surface consisting of a rounded octahedron with convex points, convex edges, and slightly concave faces, centered in the first zone.

<sup>29</sup> An extensive list may be found in Ref. 8.

Since the Fermi surface of Pb consists of only these two pieces, one would expect to see only two energy gaps in superconducting Pb, by the arguments of the preceding paragraphs. This assumption appears to be further reinforced by the fact that both pieces of the surface are smoothly shaped, but with far different mean radii of curvature. Rochlin and Douglass,<sup>17,18</sup> however, have reported observing as many as seven Pb energy gaps on a single sample by the method of superconductive tunneling.

In order to resolve this difficulty, a new calculation of the energy-gap anisotropy has recently been performed by Bennett.<sup>4</sup> His calculation is based on the premise that the anisotropy of the phonon spectrum is the principle source of the energy-gap anisotropy. The band-structure effects are then considered as a perturbation which is appreciable only near the boundaries of the Brillouin zone.

In order to illustrate how the phonon effects enter the calculation of the energy gap, we begin with the usual expression for the gap, which is given by the nonlinear integral equation<sup>1</sup>

$$\Delta_k = \sum_{k'} \frac{V_{kk'} \Delta_{k'}}{2E_{k'}}, \quad (3.1)$$

where  $\Delta_k$  represents the energy gap, and the quasiparticle energy is given by  $E_k = (\epsilon_k^2 + \Delta_k^2)^{1/2}$ , with  $\epsilon_k$  being the energy of the one-electron state designated by  $\mathbf{k}$ .<sup>30</sup> The interaction must be decomposed into

$$V_{kk'} = V_{kk'}^{\text{phonon}} + V_{kk'}^{\text{coulomb}}. \quad (3.2)$$

In the case of a superconductor, the effective electron-electron interaction via phonon exchange,  $V_{kk'}^{\text{phonon}}$ , is best represented by the Eliashberg<sup>31,32</sup> equation

$$V_{kk'}^{\text{ph}} = \frac{2(E_{k'} + \hbar\omega_{\mathbf{k}-\mathbf{k}'}) |g_{\mathbf{k}\mathbf{k}'\lambda}|^2}{(E_{k'} + \hbar\omega_{\mathbf{k}-\mathbf{k}'})^2 - E_k^2}. \quad (3.3)$$

$E_k$  and  $E_{k'}$  are quasiparticle energies,  $\hbar\omega_{\mathbf{k}-\mathbf{k}'}$  is the energy of a phonon of wave vector  $(\mathbf{k}-\mathbf{k}')$ , and  $g_{\mathbf{k}\mathbf{k}'\lambda}$  is the matrix element which couples states  $\mathbf{k}$  and  $\mathbf{k}'$  via a phonon of energy  $\hbar\omega_{\mathbf{k}-\mathbf{k}'}$  whose mode and polarization are designated by  $\lambda$ . From the structure of Eq. (3.3) it is apparent that an anisotropic phonon spectrum will lead to an anisotropic solution for  $V_{kk'}^{\text{ph}}$  via  $\hbar\omega_{\mathbf{k}-\mathbf{k}'}$ . Another possible source of anisotropy in the interaction is the anisotropy of  $g_{\mathbf{k}\mathbf{k}'\lambda}$ , which is usually taken to be isotropic for ease of calculation and replaced in the equations by its mean value.

Bennett has demonstrated that, to lowest order, the anisotropic part of the energy gap is dependent only on the anisotropy of  $V_{kk'}^{\text{ph}}$ , which in turn reflects only the

<sup>30</sup> In the BCS model, both the interaction  $V_{kk'}$  and the energy gap  $\Delta_{k'}$  are taken to be constant for  $|\epsilon_k|, |\epsilon_{k'}| < k_B\theta_D$ , so that the energy gap is a function of neither  $\mathbf{k}$  nor  $E_k$ .

<sup>31</sup> G. M. Eliashberg, Zh. Eksperim. i Teor. Fiz. **38**, 966 (1960) [English transl.: Soviet Phys.—JETP **11**, 696 (1960)].

<sup>32</sup> S. H. Liu, Phys. Rev. **125**, 1244 (1962).

anisotropy of the phonon spectrum. Because of the strong-coupling nature of Pb, however, the expression of Eq. (3.1) cannot be used to calculate the anisotropy. It is necessary in this case to use the Nambu-Gor'kov<sup>33,34</sup> Green's-function formalism, together with the Eliashberg interaction of Eq. (3.3). This approach allows the inclusion of the retardation and damping effects which arise owing to the strong electron-phonon coupling. Using this formalism, together with the known phonon dispersion curves<sup>9</sup> and average electron-phonon coupling constants<sup>5,6</sup> of Pb, Bennett has calculated the anisotropy of the energy gap in superconducting Pb by taking the isotropic solutions of the Nambu-Gor'kov-Eliashberg equations obtained by Swihart<sup>35</sup> and performing a successive iteration on them. The results of his calculation, without the effects of band structure, are shown in Fig. 3 in a (110) plane through the center of the zone. This calculation was performed for the free-electron sphere. When the actual Fermi surface was inserted into the calculation, the results were modified only in the regions where the Fermi surface appreciably deviated from this sphere, which is only over about 10% of the surface. The effects of this band structure on the gap calculation are shown in Fig. 4, which shows that the gap is modified primarily in the region of the zone boundaries, as anticipated.

Transforming from the usual  $(k_x, k_y, k_z)$  representation to an energy representation  $(\epsilon, \theta, \phi)$ , we may express these results as a two-dimensional "energy-gap surface" which represents the magnitude of the energy gap  $\Delta(\epsilon, \theta, \phi)$  at  $\epsilon=0$ <sup>36</sup> as a function of the azimuthal and polar angles  $\theta$  and  $\phi$ .

The consequences of the topology of such a surface lead to very interesting effects on the effective density of states for superconductive tunneling, as we shall discuss in Sec. IV.

Any calculation of the observable effects of energy-gap anisotropy must consider the effect of the electronic mean free path  $l$ . Whenever scattering times become very short, we must apply the theory<sup>37</sup> of "dirty" superconductivity. In this case the Bloch wave functions of the pure metal must be replaced with exact, normalized, scattered-electron eigenfunctions. This is equivalent to averaging the interaction  $V_{kk'}$ <sup>ph</sup> over the Fermi surface. The solution to the Nambu-Gor'kov-Eliashberg equations will then yield an isotropic energy gap, demonstrating that the BCS model is most applicable in the extreme dirty limit. The dirty-superconductor theory should become applicable in the regime where the

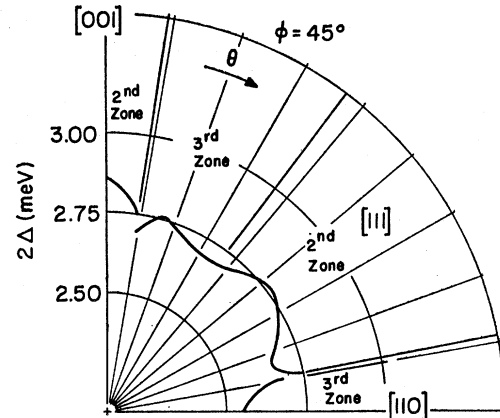


Fig. 4. The double energy gap of Pb in the (110) plane through  $\Gamma$ , with the effects of the actual band structure included (from Ref. 4).

energy uncertainty  $\hbar/\tau \approx \Delta$ , which is equivalent to setting the mean free path equal to the coherence length  $\xi_0$ . Therefore for  $l \lesssim \xi_0$  we should observe no anisotropy, but only a single gap.

In the case of thin-film tunneling junctions, the mean free path may be reduced below the bulk value,  $\approx 800 \text{ \AA}$ , of  $\xi_0$  by the effects of impurities, strain, or lack of crystal structure, exactly as in the bulk material. In addition, however, the thickness of the film acts to limit the mean free path as well. Cody and Miller<sup>38</sup> have determined that the correct relation for the mean free path of thin Pb films is  $l \approx 2d$ , where  $d$  is the film thickness, by measuring the superconducting transition in a perpendicular magnetic field. Their result agrees well with the ratio  $l \approx 8d/3$  which has been estimated from thin-film surface scattering.<sup>39</sup>

#### IV. STRUCTURE IN THE ORDINARY TUNNELING CHARACTERISTIC

##### A. Theory

The original microscopic treatment of the case of tunneling between two superconductors was an extension of the tunneling Hamiltonian formalism<sup>40</sup> which was used by Cohen, Falicov, and Phillips<sup>41,42</sup> (CFP) to explain the current-voltage characteristics of superconductor-normal-metal junctions. When this theory is extended to the two-superconductor case, complications arise because of the omission of the Cooper-pair transfer terms which are present in the

<sup>33</sup> Y. Nambu, Phys. Rev. **117**, 648 (1960).

<sup>34</sup> L. P. Gor'kov, Zh. Eksperim. i Teor. Fiz. **34**, 735 (1958) [English transl.: Soviet Phys.—JETP **7**, 505 (1958)].

<sup>35</sup> These are essentially the same as those of Ref. 53.

<sup>36</sup> For our purposes we may ignore the energy dependence of the gap. Note that  $\epsilon=0$  means  $E=\Delta$ , so that we work here only with quasiparticles at the gap edge, where the density of states is very high.

<sup>37</sup> P. W. Anderson, J. Phys. Chem. Solids **11**, 26 (1959).

<sup>38</sup> G. D. Cody and R. E. Miller, Phys. Rev. Letters **16**, 697 (1966).

<sup>39</sup> V. L. Newhouse, *Applied Superconductivity* (John Wiley & Sons, Inc., New York, 1964), p. 108.

<sup>40</sup> J. Bardeen, Phys. Rev. Letters **6**, 57 (1961); **9**, 147 (1962).

<sup>41</sup> M. H. Cohen, L. M. Falicov, and J. C. Phillips, Phys. Rev. Letters **8**, 316 (1962).

<sup>42</sup> R. E. Prange, Phys. Rev. **131**, 1083 (1963).

microscopic theory. Josephson<sup>43,44</sup> and others<sup>45-47</sup> have shown that a proper treatment leads to additional terms in the tunneling current. These give rise to a host of interesting properties, known under the collective heading of the Josephson effect, which we shall discuss in the next two sections.

For the present, however, we shall restrict ourselves to those effects which arise from the single-particle terms in the tunneling equation. We may then extend the CFP equations directly to the two-superconductor case.

In the CFP formalism, taking  $T_{\mathbf{k}\mathbf{q}}$  as a matrix element connecting states  $\mathbf{k}$  and  $\mathbf{q}$  on opposite sides of the barrier, time-dependent perturbation theory expresses the current through the barrier as

$$I = \frac{4\pi e}{\hbar} \sum_{\mathbf{k}, \mathbf{q}} |T_{\mathbf{k}\mathbf{q}}|^2 [f(E_{\mathbf{k}}) - f(E_{\mathbf{q}})] \delta(E_{\mathbf{k}} - E_{\mathbf{q}} + eV). \quad (4.1)$$

In this expression  $V$  is the voltage across the junction (always taken to be applied to metal 2),  $f$  is the Fermi distribution function, and the summation over the spins has been performed trivially. Placing this in integral form we obtain<sup>48-51</sup>

$$I = \frac{4\pi e}{\hbar} \sum_{k_t, q_t} \int dE_{\mathbf{k}} \int dE_{\mathbf{q}} |T_{\mathbf{k}\mathbf{q}}|^2 \rho_1(E_{\mathbf{k}}) \rho_2(E_{\mathbf{q}}) \times [f(E_{\mathbf{k}}) - f(E_{\mathbf{q}})] \delta(E_{\mathbf{k}} - E_{\mathbf{q}} + eV), \quad (4.2)$$

where  $\rho_1$  and  $\rho_2$  are the densities of states in metals 1 and 2, respectively, while  $k_t$  and  $q_t$  are the wave-vector components tangential to the barrier.

In the single-crystal case, Eq. (4.2) selects only those parts of the Fermi surface for which the electron group velocity  $\mathbf{v}_{\mathbf{k}}$  is almost perpendicular to the barrier.<sup>52</sup>

<sup>43</sup> B. D. Josephson, Phys. Letters **1**, 251 (1962).

<sup>44</sup> B. D. Josephson, Advan. Phys. **14**, 419 (1965).

<sup>45</sup> P. W. Anderson, *Lectures on the Many Body Problem* (Academic Press Inc., New York, 1963), Vol. 2.

<sup>46</sup> R. A. Ferrel and R. E. Prange, Phys. Rev. Letters **10**, 479 (1963); Phys. Rev. Letters **11**, 104(E) (1963).

<sup>47</sup> V. Ambegaokar and A. Baratoff, Phys. Rev. Letters **10**, 486 (1963).

<sup>48</sup> R. Stratton, J. Phys. Chem. Solids **23**, 1177 (1962).

<sup>49</sup> R. Stratton, Phys. Rev. **136**, A837 (1964).

<sup>50</sup> T. E. Hartman, J. Appl. Phys. **35**, 3283 (1964).

<sup>51</sup> W. A. Harrison, Phys. Rev. **123**, 85 (1961).

<sup>52</sup> The boundary conditions for the transverse  $k$ -vector summation have been studied in detail by Stratton [Refs. 48 and 49]. For the case of specular transmission he derives

$$|T_{\mathbf{k}\mathbf{q}}|^2 = [4\pi^2 N_1(E_{\mathbf{k}}) N_2(E_{\mathbf{q}})]^{-1} e^{-\zeta}.$$

Taking the  $x$  direction to be perpendicular to the barrier, we have

$$\zeta = \frac{2(2m)^{1/2}}{\hbar} \int_{x_1}^{x_2} [\varphi(x) + E_f - E_x]^{1/2} dx.$$

Here  $\varphi(x)$  is the barrier potential measured from the Fermi level  $E_f$ ,  $x_1$  and  $x_2$  are the classical turning points, where the energy of the electron is given by  $E_x = \hbar^2 k_x^2 / 2m$  [Ref. 50]. This result is identical to that derived by Harrison [Ref. 51] using the WKB approximation. [Although the insertion of diffuse boundary conditions modifies the integrand of Eq. (4.2) somewhat, the  $e^{-\zeta}$  factor with which we are most concerned remains unaltered.] Taking a free-electron approximation for the Fermi surface, we

For a complex Fermi surface, however, it is possible that there will be several different parts of the surface for which this condition is satisfied. Under such conditions several energy gaps may be observed in a single crystal direction.<sup>8,20-22</sup>

The samples used in these experiments, however, were constructed with Pb films of a highly polycrystalline nature. In this case we must average over all contributions from variously oriented crystallites. Such an averaging may be approximated by assuming that all crystallographic directions contribute equally. This is equivalent to replacing  $|T_{\mathbf{k}\mathbf{q}}|^2$  in Eq. (4.2) with an average matrix element  $|T|^2$  which is independent of energy. In the following discussion we take the convention that  $E_f = 0$  in the absence of applied voltage, and assume that we are working only with energies very close to  $E_f$ , so that we may replace the normal-state density of states  $N(E)$  with its value at the Fermi surface; i.e.,  $N(0)$ . Since we wish to average over all directions, we also delete the sum over  $k_t$  and  $q_t$ , obtaining the usual tunneling expression

$$I \propto |T|^2 \int_{-\infty}^{+\infty} dE \rho_1(E) \rho_2(E + eV) \times [f(E) - f(E + eV)]. \quad (4.3)$$

The effective density of states for tunneling may be expressed in the form

$$\rho(E) = \frac{N(0)}{4\pi} \int_{-1}^{+1} d(\cos\theta) \times \int_0^{2\pi} d\phi \operatorname{Re} \left\{ \frac{E}{[E^2 - \Delta^2(E, \theta, \phi)]^{1/2}} \right\}. \quad (4.4)$$

As we are concerned only with structure near the peak in  $\rho(E)$  we may neglect<sup>56</sup> the energy dependence<sup>53</sup> of  $\Delta$  and use  $\Delta = \Delta(\theta, \phi)$  to a good approximation.

Following Bennett, we define an "energy-gap distribution function"  $g(x)$  such that

$$g(x) = \frac{1}{4\pi} \int_{-1}^{+1} d(\cos\theta) \int_0^{2\pi} d\phi \delta[x - \Delta(\theta, \phi)]. \quad (4.5)$$

Therefore, the equation for  $\rho(E)$  becomes<sup>54</sup>

$$\rho(E) = N(0) \int_{x_{\min}}^E \frac{E}{(E^2 - x^2)^{1/2}} g(x) dx. \quad (4.6)$$

may replace  $E_x$  with the expression  $E_x = E_f \cos^2\theta$ , where  $\theta$  is the angle between the normal to the barrier and the group velocity,  $\mathbf{v}_{\mathbf{k}} = \hbar^{-1} \nabla_{\mathbf{k}} E_{\mathbf{k}}$ , of the tunneling electron. Using typical junction parameters [ $d \approx 20 \text{ \AA}$ ,  $\varphi(x) \approx 1 \text{ eV}$ ,  $E_f \approx 10 \text{ eV}$ ],  $e^{-\zeta}$  drops to  $\frac{1}{2}$  of the normal incidence value when the group velocity lies in a direction approximately  $5^\circ$  away from perpendicular to the barrier. This sharp selectivity does not appreciably alter even in the extreme diffuse scattering limit.

<sup>53</sup> J. R. Schrieffer, D. J. Scalapino, and J. W. Wilkins, Phys. Rev. Letters **10**, 336 (1963).

<sup>54</sup> A calculation of  $\rho(E)$  for a model anisotropic superconductor is given in Appendix A.

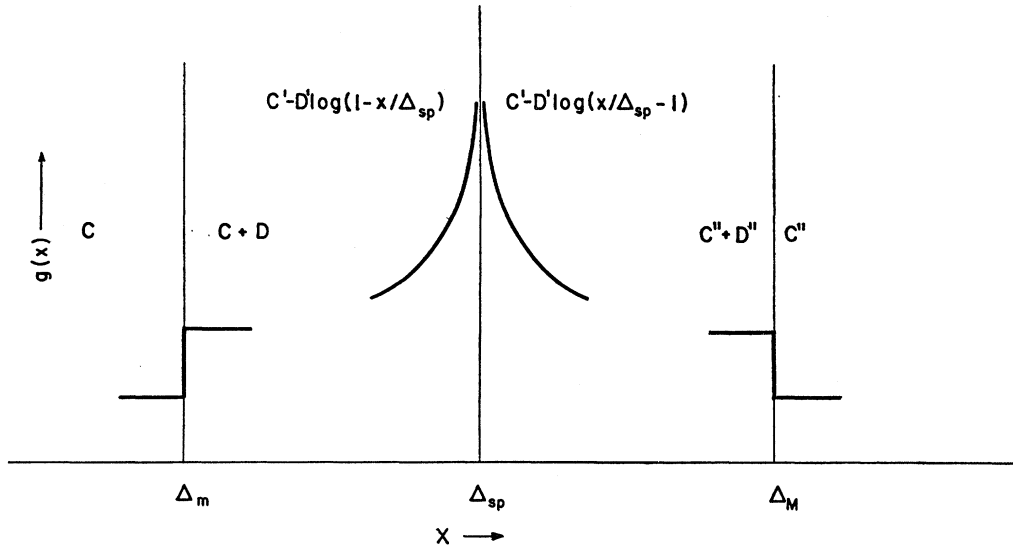


FIG. 5. The form of the energy-gap distribution function  $g(x)$  in the vicinity of the three types of critical values of the anisotropic energy gap.  $\Delta_m$  is a minimum,  $\Delta_{sp}$  a saddle point, and  $\Delta_M$  a maximum.

For an isotropic superconductor  $\Delta = \text{constant}$  and, therefore,

$$g(x) = \delta(x - \Delta), \quad (4.7)$$

which gives the correct expression for the superconducting density of states in an isotropic superconductor,

$$\rho(E) = N(0) \operatorname{Re} \left[ \frac{E}{(E^2 - \Delta^2)^{1/2}} \right]. \quad (4.8)$$

Bennett has pointed out that in the case of Pb the two-dimensional Van Hove<sup>55</sup> theorems apply to  $g(x)$ . This property can then be used to study the effect on  $\rho(E)$  of the "critical values"  $\Delta_c$  of the energy-gap surface; that is, the value of the anisotropic gap at those points for which  $\Delta(\theta, \phi)$  is a local maximum, minimum, or saddle point. The form of  $g(x)$ , expanded about  $\Delta_c$ , for these three types of critical values, is illustrated in Fig. 5.

Inserting these formulas for  $g(x)$  into Eq. (4.6) and performing the integration then yields the form of  $\rho(E)$  and  $d\rho(E)/dE$ , expanded about  $\Delta_c$ , corresponding to the three types of critical values. As shown in Table I, we have found  $\rho(E)$  to be everywhere continuous, while  $d\rho(E)/dE$  has square-root singularities for  $E \sim \Delta_m^+$ ,  $E \sim \Delta_M^+$ , and  $E \sim \Delta_{sp}^-$ . We find no singularity for  $E \sim \Delta_{sp}^+$ , in contrast to the results quoted in Ref. 4.<sup>56</sup> These expressions were subsequently inserted into the tunneling equation in order to study the effect of the anisotropy on the junction tunneling characteristic.

Returning to the two-superconductor case we set  $T = 0^\circ\text{K}$  in Eq. (4.3) to obtain

$$I \propto |T|^2 \int_{-eV}^0 dE \rho_1(E) \rho_2(E + eV). \quad (4.9)$$

For the case of the two-isotropic-superconductor junc-

TABLE I. The leading terms of  $\rho(E)$  and  $d\rho(E)/dE$  for an anisotropic superconductor when  $E$  is in the vicinity of a critical value  $\Delta_c$  of  $\Delta(\theta, \phi)$ .  $A$  and  $B$  are constants which depend on the details of the gap distribution function  $g(x)$ .

Type of critical value	$\rho(E)$		$d\rho(E)/dE$	
	$E \leq \Delta_c$	$E \geq \Delta_c$	$E \leq \Delta_c$	$E \geq \Delta_c$
Minimum ( $\Delta_m$ )	$\frac{\pi}{2} A E$ (continuous)	$\frac{\pi}{2} (A+B) E - B E \sin^{-1} \left( \frac{\Delta_m}{E} \right)$	$\frac{\pi}{2} A$	$B \left( \frac{\Delta_m}{2} \right)^{1/2} (E - \Delta_m)^{-1/2}$
Saddle point ( $\Delta_{sp}$ )	$A' E - 2\pi B' \Delta_{sp}^{1/2} (\Delta_{sp} - E)^{1/2}$	$A' E$ (continuous)	$\pi B' \Delta_{sp}^{1/2} (\Delta_{sp} - E)^{-1/2}$	$A'$
Maximum ( $\Delta_M$ )	$\frac{\pi}{2} (A'' + B'') E$ (continuous)	$\frac{\pi}{2} B'' E + A'' \sin^{-1} \left( \frac{\Delta_M}{E} \right)$	$\frac{\pi}{2} (A'' + B'')$	$-A'' \left( \frac{\Delta_M}{2} \right)^{1/2} (E - \Delta_M)^{-1/2}$

<sup>55</sup> L. Van Hove, Phys. Rev. 89, 1189 (1953).

<sup>56</sup>  $\rho(E)$  and  $d\rho(E)/dE$  are quoted in Ref. 4 as  $dI/dV$  and  $d^2I/dV^2$  for a superconductor-normal metal junction. The error in  $\rho(E)$  affects all succeeding line-shape calculations in Ref. 4 which involve  $\Delta_{sp}^+$ .

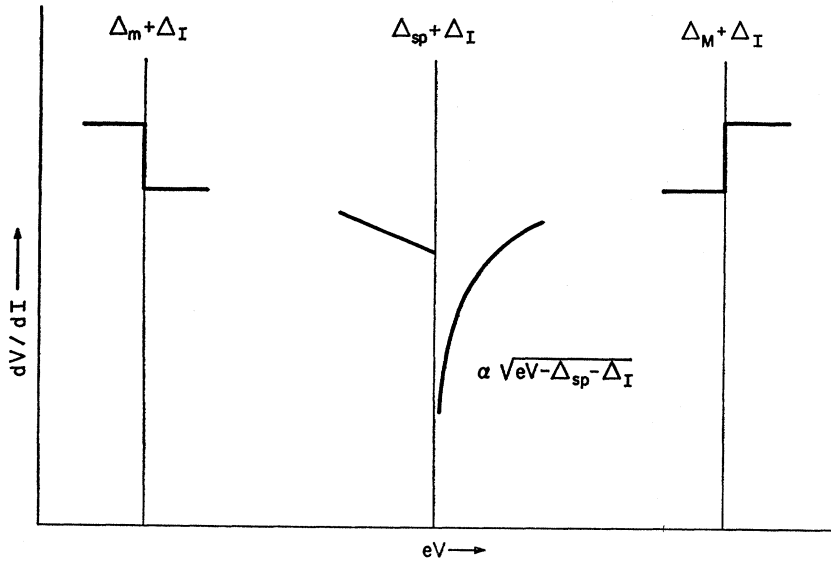


FIG. 6. Theoretical  $dV/dI$  line shapes for an anisotropic superconductor-isotropic superconductor junction, for  $eV$  in the vicinity of  $\Delta_I + \Delta_{2c}$ , where  $\Delta_I$  is the energy gap of the isotropic superconductor. The three cases for  $\Delta_{2c}$  are:  $\Delta_m$ , a minimum;  $\Delta_{sp}$ , a saddle point; and  $\Delta_M$ , a maximum.

tion the insertion of Eq. (4.8) into Eq. (4.9) results in the expression

$$I = P \int_{-eV}^0 dE \frac{E(E+eV)}{(E^2 - \Delta_1^2)^{1/2} [(E+eV)^2 - \Delta_2^2]^{1/2}}, \quad (4.10)$$

where  $P$  is not a function of  $N(0)$ . The properties of Eq. (4.10) are well known, the most interesting one being the jump discontinuity in  $I$  at  $eV = \Delta_1 + \Delta_2$ .

Of somewhat greater experimental interest are the derivatives  $dV/dI$  and  $d^2V/dI^2$  of the tunneling characteristic, which yield a great deal more information about the structure of the gap function than the  $I$ - $V$  curve itself. In the isotropic-isotropic case,  $dV/dI$  is given by a Dirac  $\delta$  function;  $dV/dI \propto [\delta(eV - \Delta_1 - \Delta_2)]^{-1}$ .

In the case of an isotropic-superconductor-anisotropic superconductor junction we take the convention that superconductor 1 is isotropic, so that

$$\rho_1(E) = E/(E^2 - \Delta_1^2)^{1/2}.$$

We have calculated the form of  $dV/dI$  and  $d^2V/dI^2$  near  $eV = \Delta_1 + \Delta_{2c}$ , where  $\Delta_{2c}$  is a critical value of  $\Delta_2(\theta, \phi)$ , by inserting the expansions of  $\rho_2(E+eV)$  about  $\Delta_{2c}$  given in Table I. An example of this calculation, for  $eV = \Delta_1 + \Delta_{2sp}$ , is given in Appendix B. The analytic forms of  $dV/dI$  in the vicinity of the three types of critical values are shown in Fig. 6.  $dV/dI$  is seen to have a step-like behavior at  $\Delta_m$  and  $\Delta_M$ ; there is a square root singularity at  $(\Delta_I + \Delta_{sp})^+$ , rather than the logarithmic singularity reported by Bennett. All of the  $dV/dI$  structure is, as expected, less singular than the single  $\delta$  function obtained for the isotropic-isotropic case.

The case of the two-identical-anisotropic-superconductor junction is somewhat more complex, as there are now six possible distinct singularities in  $dV/dI$  to examine, with both  $\rho_1(E)$  and  $\rho_2(E+eV)$  being given by the expressions of Table I. As this case is of some-

what less experimental interest, it is sufficient to note that we have found  $dV/dI$  to be *everywhere continuous* for the anisotropic-anisotropic junction. A calculation of this type for  $eV = 2\Delta_{sp}$  is also given in Appendix B.

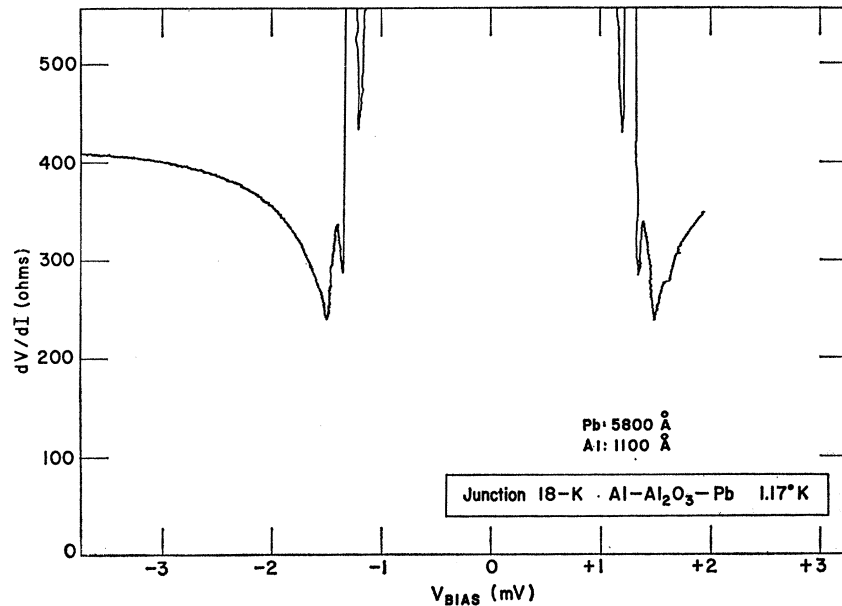
## B. Experiment

The differential-resistance ( $dV/dI$ )-versus-dc-bias-voltage ( $V$ ) characteristics of a variety of tunnel junctions were measured by the small-signal ac technique. In some cases the second derivative ( $d^2V/dI^2$ ) characteristic was also taken, by measuring the second harmonic of the applied ac voltage. In all the junctions used at least one of the two metals was a Pb film, which we shall refer to as the anisotropic superconductor ( $S_a$ ). The junctions may then be divided into three categories according to whether the second metal is normal ( $S_a$ - $I$ - $N$  junction), an isotropic superconductor ( $S_a$ - $I$ - $S_i$  junction), or another Pb film ( $S_a$ - $I$ - $S_a$  junction). Owing to the differences among these cases in both experimental results and theoretical calculations we shall discuss them separately.

### $S_a$ - $I$ - $S_i$ Case

Junctions of this type were all of the construction Pb- $I$ -Al, where the insulating layer was usually obtained by oxidation of the Al film. The effects of thermal broadening are expected to be minimal in this case, even at temperatures close to  $T_c(\text{Al})$ . This is due to the fact that the comparatively sharp density-of-states peak in the Al acts as a narrow probe for the investigation of the structure of the energy gap in the Pb film. An equivalent mathematical formulation of this statement is that we may take the limits of integration in, for example, Eq. (B1) quite close together, even at finite temperatures.

FIG. 7. The  $dV/dI$  characteristic of a Pb-I-Al junction exhibiting structure at  $\Delta_{\text{Pb}} + \Delta_{\text{Al}} = \pm 1.3$  to 1.6 mV which is due to the anisotropy of the Pb gap. The sharp spike at  $\pm 1.2$  mV is part of the  $\Delta_{\text{Pb}} - \Delta_{\text{Al}}$  structure.



Our Al films were  $\lesssim 1000$  Å thick in these samples. As the bulk coherence length is  $\approx 15\,000$  Å for Al, the Al films were always in the “dirty” limit of the Anderson theory, yielding a single BCS-like energy gap. The Pb films varied in thickness from  $(d/\xi_0)_{\text{Pb}} \lesssim 1$  to  $(d/\xi_0)_{\text{Pb}} \approx 7$ , corresponding to mean-free-path/coherence-length ratios varying from 2 to 14.

For thick Pb films, we have observed structure in the vicinity of the sum of the energy gaps of the two superconductors which arises from the anisotropy of the Pb energy gap. Such structure is shown in Fig. 7. The sharpening of this fine structure as the temperature was lowered through  $T_c(\text{Al})$ , as shown in Fig. 8, illustrates how the rapidly sharpening peak in the Al density of states effectively “short circuits” the temperature broadening due to the Fermi factors. The fact that this structure remains at fixed voltage intervals as we go from  $T_c(\text{Al})$  down to the lowest temperatures reached proves that it arises from structure on the Pb density of states, and is not related to the Al. Figure 9 shows how sharp the structure becomes at the lowest temperature reached. The equivalent energy of the structure on the Pb density of states which causes the effects shown was determined by carefully following both  $\Delta_{\text{Pb}} + \Delta_{\text{Al}}$  and  $\Delta_{\text{Pb}} - \Delta_{\text{Al}}$  as a function of temperature, and subsequently subtracting the value of  $\Delta_{\text{Al}}$  from the measured voltage of the sum.

No structure has been observed by this method for Pb films whose thickness was less than  $4\xi_0$ . It has also been noted that severe thermal cycling, such as rapid removal of the sample from the He bath, causes the structure observed in the thick-film junctions to disappear when the junctions are immediately remeasured. If, however, the sample is allowed to remain for several weeks at room temperature following such a cycle, the

anisotropy structure is again present on the junction characteristics when the sample is remeasured. For these reasons we believe that the samples showing anisotropy effects are relatively strain-free as prepared, so that the mean free path is, indeed, effectively thickness limited. This will in general only be true in films having a polycrystalline structure, with crystallites at least of the order of the film thickness in transverse dimension. If this were not the case, the mean free path would be of the order of the crystallite dimensions rather than having any correlation with the thickness of the films. It is also interesting to note that a thick-film sample which has exhibited no anisotropy effects the first time it is measured has never shown any such effects

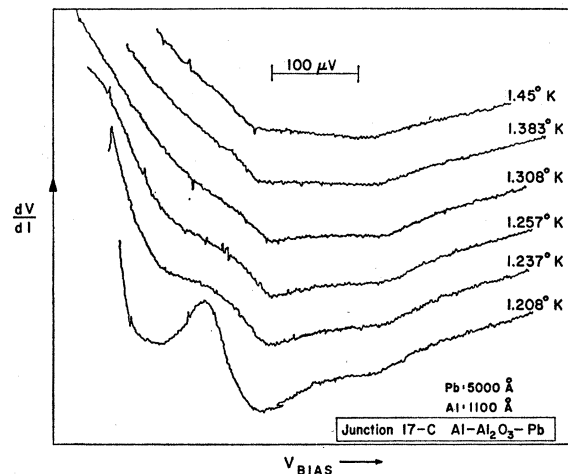


FIG. 8. The  $dV/dI$  characteristic of a Pb-I-Al junction near  $eV = \Delta_{\text{Pb}} + \Delta_{\text{Al}}$ , illustrating the growth of the anisotropy effects out of the background as the Al gap opens up. The curves have been displaced vertically for clarity.

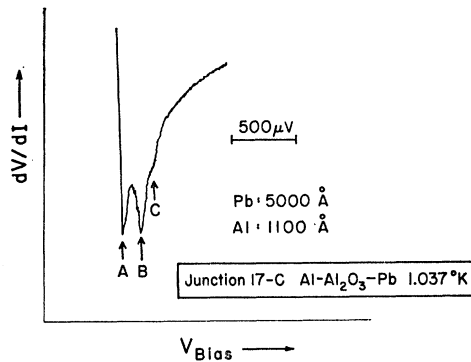


FIG. 9. The  $dV/dI$  characteristic of a Pb-I-Al junction at low temperatures, in the vicinity of  $eV = \Delta_{\text{Pb}} + \Delta_{\text{Al}}$ . The spike at A may be compared with the predicted line shape for a saddle point, as shown on Fig. 6. The shoulder at C may similarly be compared with the predicted line shape for a maximum, superimposed on a rapidly varying background. Although the structure at B resembles a saddle point, it is present even on thin or "dirty" samples, and arises from the "average" value of the Pb energy gap.

at a later remeasurement, no matter how long it has been allowed to anneal at room temperature. From this we infer that the crystallization of the films occurs during deposition, and that no recrystallization occurs during the room-temperature annealing process. Thus the effects of thermal cycling are probably due to induced strain in the films, rather than a destruction of crystallite structure.

#### $S_a$ -I- $S_a$ Case

These junctions were all of the form Pb-I-Pb, the oxide layer having been grown at 50°C in a pure oxygen atmosphere. They showed no structure in the vicinity of  $eV = 2\Delta_{\text{Pb}}$ , which could be attributed to anisotropy effects, even for films whose thickness greatly exceeded the coherence length.

This somewhat surprising result may be easily understood by examining the form of  $\rho(E)$  for an anisotropic superconductor given in Table I. It can be seen from this table that the effect of the anisotropy is to remove the square-root singularity of the isotropic case from the density of states, and smear it out into a non-singular function over the range of anisotropy values.<sup>57</sup> As we have pointed out, the result of this smearing of the density-of-states function is, in this case, to make  $dV/dI$  a continuous nonsingular function of  $V$ . Additionally, the lack of any sharp singularity in  $\rho(E)$  allows the effects of finite temperature to enter fully, contrary to the case of the  $S_a$ -I- $S_i$  junction discussed previously. Since the integration for the current, which includes the thermal broadening, must be performed *before* taking the derivatives, the predicted  $T=0^\circ\text{K}$  structure in  $d^2V/dI^2$  should become smeared out even at 1°K. Because of difficulties in sample preparation we were not

<sup>57</sup> An example of this "smearing" is exhibited in the model calculation of Appendix A.

able to construct a junction for which one of the Pb films was thin, so that all of our Pb-I-Pb junctions fell into the two-anisotropic-superconductor category.

#### $S_a$ -I- $N$ Case

Junctions of this type were either of the composition Pb-I-Mg or were the Pb-I-Al junctions mentioned before, but measured above  $T_c(\text{Al})$ . A large number of such junctions were measured, with Pb thicknesses ranging from less than 800 Å to over 6000 Å. No structure was observed in either the first or second derivatives of the characteristics of the Pb-I-Mg junctions at any temperature down to 1.04°K. No structure was observed at temperatures above  $T_c(\text{Al})$  on any Pb-I-Al junction, even on those junctions which *do* exhibit structure due to anisotropy *below*  $T_c(\text{Al})$ .

For this type of junction, at  $T=0^\circ\text{K}$ , one obtains the well-known formula  $dV/dI \propto 1/\rho(E)$ . The lack of observed singularities in  $dV/dI$  on such junctions is in agreement with our calculation of  $\rho(E)$ . The thermal broadening of the normal-metal density of states at 1°K,  $4k_B T \approx 350 \mu\text{eV}$ , is sufficient to account for the complete lack of detail in the  $dV/dI$  characteristic, which washes out the possible  $d^2V/dI^2$  singularities.

#### Summary

To sum up the experimental observations, the only case for which the anisotropy of the Pb energy gap is observed in the ordinary tunneling characteristic is that of the  $S_a$ -I- $S_i$  junction. We have examined many such junctions in detail, and have compared the results with the theoretical line-shape calculations in order to identify the type of critical value of the gap associated with each of the various structures.

#### C. Results

The  $dV/dI$  characteristic of a typical (thick Pb)-I-Al junction, at the lowest temperature obtained, in the vicinity of  $V = (\Delta_{\text{Al}} + \Delta_{\text{Pb}})/e$ , is shown in Fig. 9. The structure of this characteristic may be compared with the theoretically derived line shapes shown in Fig. 6. The sharp spike at point A, for instance, is virtually identical to the predicted line shape for  $dV/dI$  in the vicinity of  $\Delta_I + \Delta_{sp}$ . The shoulder at point C is, when the background is subtracted out, exactly like the predicted step for  $dV/dI$  in the vicinity of  $\Delta_I + \Delta_M$ . By comparing in this manner, we have been able to identify structure due to a critical value as arising from either a relative maximum or a saddle point on the energy-gap surface. The equivalent energy of these critical values has been carefully measured, and the results summarized in Table II. No minima were observed.

There is some doubt about the nature of the observed structure at 2.71 meV, as this is the value of the averaged energy gap observed in "dirty" Pb films. The pres-

TABLE II. Critical values,  $2\Delta_c$ , of the anisotropic energy gap of superconducting Pb (in meV), as determined from analysis of Pb-I-Al junctions. All values are extrapolated to  $T=0^\circ\text{K}$ .

Substrate number <sup>a</sup> Pb thickness, $\pm 10\%$ ( $\text{\AA}$ )	7 <sup>b</sup> 800	14 3500	17 5000	18 5800
(Saddle point)	...	$2.45 \pm 0.02$	$2.43 \pm 0.02$	$2.43 \pm 0.02$
(Saddle point)	...	$2.55 \pm 0.02$	...	...
[Average gap] <sup>c</sup> (Maximum)	$[2.72 \pm 0.02]$ ...	$[2.72 \pm 0.02]$ ...	$[2.70 \pm 0.02]$ $2.98 \pm 0.02$	$[2.71 \pm 0.01]$ $2.99 \pm 0.02$

<sup>a</sup> Several junctions were measured on each substrate. All gave identical results.

<sup>b</sup> This junction has  $d \approx \xi_0$ , so that no anisotropy is expected.

<sup>c</sup> This is the "average" gap, and not a critical value (see text).

ence of amorphous or badly strained regions in the junction area would give rise to a  $dV/dI$  minimum at this value whose structure would closely resemble that of a saddle-point critical value.

The lack of structure due to the absolute minimum of the gap surface is evidently due to its having an energy sufficiently small that it lies buried in that part of the characteristic which arises from the difference of the energy gaps. No such minimum could be identified on any of our junctions, despite a careful and most thorough search for its presence.

Some structure was also observed on the difference peak, for Pb-I-Al junctions, but this was never as well resolved as the structure at the sum of the gaps. For this reason, and also because the amplitude of the difference peak diminishes rapidly with temperature, these data were decidedly inferior in quality to those obtained at the sum, and have not been tabulated in this work. Such data as could be obtained agreed very well with the results of Table II.

## V. SUBHARMONIC STRUCTURE

### A. Experiment

For a junction composed of two identical superconductors, ordinary tunneling theory predicts, at low temperatures, a very small temperature-dependent current for small bias voltages, followed by an abrupt current rise as the bias is increased to  $eV=2\Delta$ . For larger biases the current goes asymptotically to the slope which would be obtained if both films were driven normal. This is consistent with the experimental observations on ordinary tunneling junctions. The ordinary excess current which flows at  $eV < 2\Delta$  is due to thermal excitation of quasiparticles, and, in addition to being strongly temperature-dependent, it is quite devoid of structure.

The first anomalous structure reported in the excess current was a sharp current step at  $eV=2\Delta/2$  followed by a rapid current rise for increasing voltage, both superimposed on the temperature-dependent background.<sup>58,59</sup> There have also been reports of structure

occurring at  $eV=2\Delta/3$ ,  $2\Delta/4$ , etc., for a variety of junctions, although most of these reports have been unpublished.

Rochlin and Douglass<sup>18</sup> have recently reported observing excess currents, having only a weak dependence on temperature, which exhibit quite pronounced structure. This structure takes the form of a series of steps in the tunneling current at bias voltages given by  $eV=2\Delta/m$ , where  $m$  is an integer. As the structure occurs at integral submultiples of the primary current step at  $eV \approx 2\Delta$ , we refer to it as "subharmonic structure" (SHS).

Early reports of SHS on Sn-I-Sn<sup>60</sup> and Pb-I-Pb<sup>61</sup> tunneling junctions described a series of broad minima in  $dV/dI$  at biases of approximately  $2\Delta/m$ . Such structure has been observed by us in Sn-I-Sn junctions, where the Sn film thicknesses were less than the coherence length. Similar structure has been observed<sup>61</sup> on Pb-I-Pb junctions whose films were of the order of the coherence length in thickness.<sup>62</sup>

We have constructed a number of Pb-I-Pb junctions, with both films thicker than the coherence length, whose characteristics exhibit a great deal of fine structure in addition to the broad SHS. The  $dV/dI$  characteristic of such a junction at  $4.22^\circ\text{K}$  is shown in Fig. 10. The broad SHS for  $m=2, 3$ , and 4 can easily be discerned on this figure, while the fine structure tends to obscure it at higher indices, i.e. lower voltages.

We find that this fine SHS falls into a number of series of  $dV/dI$  minima occurring at exactly  $V_c/m$ , where  $V_c$  is a voltage of the order of  $2\Delta_{\text{Pb}}/e$ .

A number of experimental observations concerning this fine structure have been assembled by studying the details of the junction characteristics as a function of both temperature and magnetic field. These are:

<sup>60</sup> I. K. Yanson, V. M. Svistunov, and I. M. Dmitrenko, Zh. Eksperim. i Teor. Fiz. 47, 2091 (1964) [English transl.: Soviet Phys.—JETP 20, 1404 (1965)].

<sup>61</sup> S. M. Marcus, Phys. Letters 19, 623 (1966); 20, 236 (1966).

<sup>62</sup> Comparing this SHS with the single step of Taylor and Burstein, it is not clear whether these structures are, in fact, related. Apropos of this statement, S. M. Marcus (private communication) has reported the simultaneous occurrence of both of these types of structure on a single junction, inferring that they arise from different mechanisms.

<sup>58</sup> B. N. Taylor and E. Burstein, Phys. Rev. Letters 10, 14 (1963).

<sup>59</sup> C. J. Adkins, Phil. Mag. 8, 1051 (1963); Rev. Mod. Phys. 36, 211 (1964).

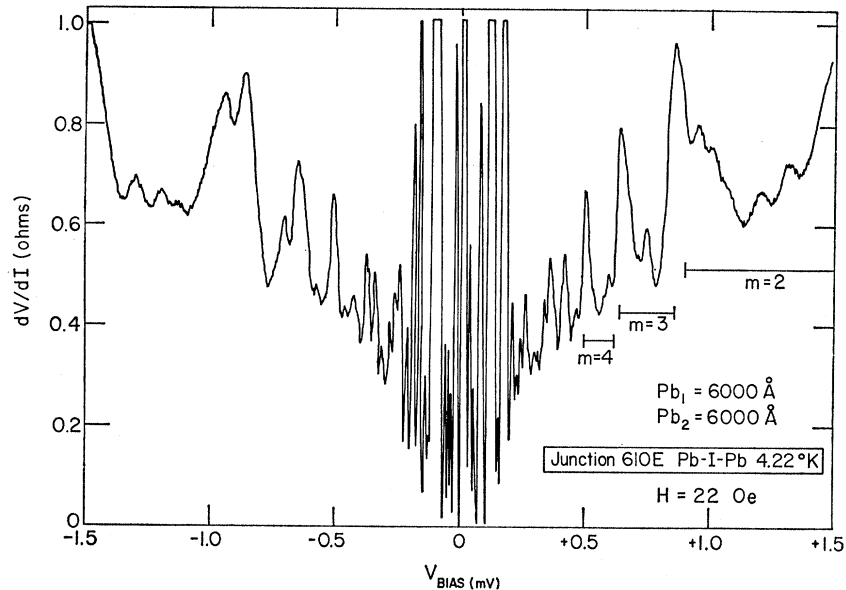


FIG. 10. The  $dV/dI$  characteristic of a Pb-I-Pb junction at 4.22°K, showing the complex fine structure in the SHS.

(1) When the temperature is lowered from 4.2°K to 1.2°K there is a 6.5% increase in the bias voltages of each of the fine-structure minima in  $dV/dI$ . This is precisely the percentage increase shown by the Pb energy gap over this range, as determined by measuring the bias voltage of the primary minimum at  $eV = 2\Delta$ . Thus the fine structure must arise from a process which directly involves the energy gap, rather than from defects in the oxide layer or defects in the films.

(2) There is a smooth temperature-dependent excess background current in addition to the structure observed. At 4.2°K this current is roughly of the same magnitude as the subharmonic current. As the temperature is lowered, the smooth background decreases very rapidly, so that for temperatures below 2°K it is essen-

tially unobservable except in the region very close to  $eV = 2\Delta$ . This background has been explained as consisting partially of the normal thermally excited quasi-particle current, and partially of the thermal-phonon assisted tunneling<sup>63</sup> which is usually observed in Pb-I-Pb junctions.

The amplitude of the structured current, however, is affected only slightly by this temperature decrease, the primary effect of going to lower temperatures being to increase the resolution of the  $dV/dI$  minima. Two factors contributing to the increasing resolution are the decrease of thermal smearing effects and the removal of the temperature-dependent background which tends to obscure fine details. Most significantly, there is no qualitative change in the detailed shape of the fine-

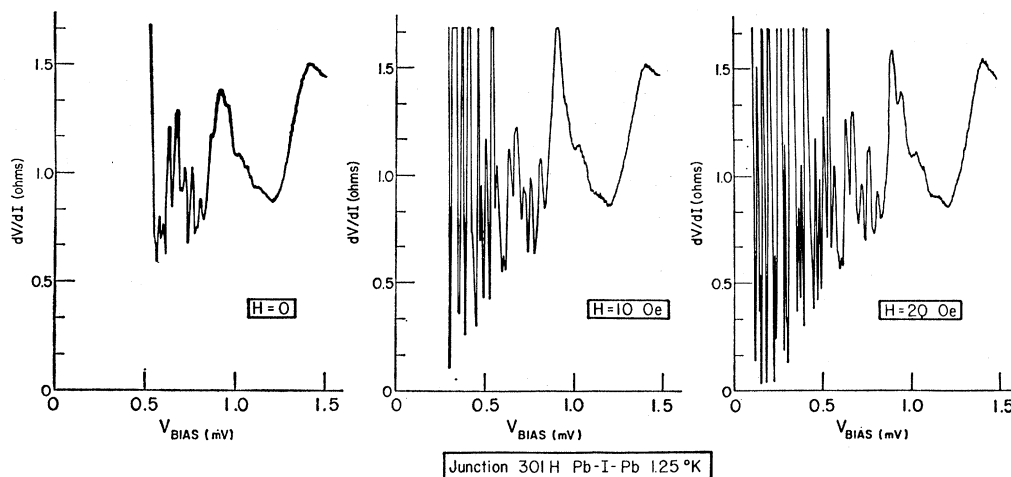


FIG. 11. The  $dV/dI$  characteristic of a Pb-I-Pb junction at 1.25°K, showing the weak dependence of the SHS on small parallel magnetic fields. The small bias region cannot be reached with a constant-current source in the presence of dc Josephson effects (cf. Fig. 13).

<sup>63</sup> L. Kleinman, B. N. Taylor, and E. Burstein, Rev. Mod. Phys. 36, 208 (1964).

FIG. 12. (a) The  $dV/dI$  characteristic of a Pb-I-Pb junction at 1.18°K. One of the  $V_c/m$  series is indicated, for  $V_c=2.31$  mV. The structure below 0.3 mV has been omitted due to its complexity. Every minimum on this figure has been fitted to such a  $V_c/m$  series. (b) The small-bias region of Fig. 12(a). The  $V_c/m$  series for  $V_c=2.31$  mV is indicated.

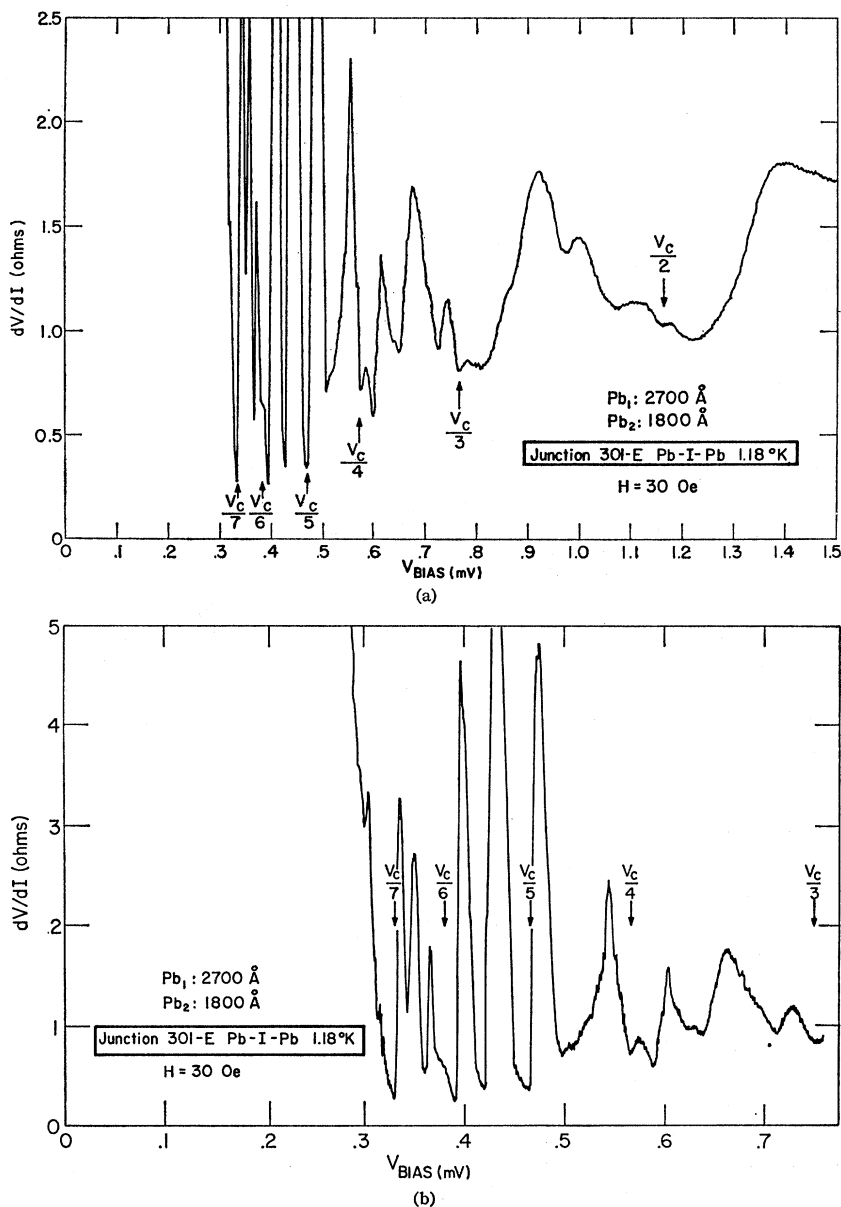


TABLE III. Experimentally determined values of  $V_c$  for Pb (in meV) as determined from SHS in Pb-I-Pb junctions. All values are extrapolated to  $T=0^\circ\text{K}$ .

Sample number	$V_c = \Delta_{1c} + \Delta_{2c}$				
	601 H	608 H	610 E	301 H	301 E
Film thicknesses $\pm 10\%$ (Å)	6000 4700	4700 2300	6000 6000	2800 1800	2800 1800
Experimentally determined $V_c$ values.	$2.11 \pm 0.02$	...	$2.11 \pm 0.02$	$2.11 \pm 0.02$	$2.15 \pm 0.02$
	...	$2.22 \pm 0.02$	$2.26 \pm 0.02$	$2.22 \pm 0.02$	...
	...	...	...	$2.34 \pm 0.02$	$2.31 \pm 0.02$
	...	...	...	$2.39 \pm 0.02$	$2.39 \pm 0.02$
	$2.44 \pm 0.02$	$2.45 \pm 0.02$	$2.44 \pm 0.02$	$2.46 \pm 0.02$	$2.44 \pm 0.02$
	...	...	...	...	$2.52 \pm 0.02$
	...	...	$2.62 \pm 0.02$	$2.62 \pm 0.02$	$2.60 \pm 0.02$
$2.97 \pm 0.02$	$2.97 \pm 0.02$	$2.96 \pm 0.02$	$2.97 \pm 0.02$	$2.92 \pm 0.02$	

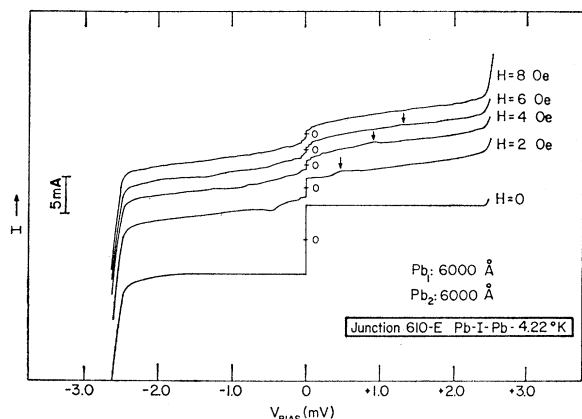


FIG. 13. The  $I$ - $V$  curves of a Pb-I-Pb junction, showing three types of phenomena due to the Josephson effect as a function of parallel magnetic field. The large current step at  $V=0$  is the dc effect; the small sharp steps very near  $V=0$  are cavity modes; the "bump" due to the travelling-wave mode, which moves towards increasing  $V$  for increasing  $H$ , is indicated by arrows. The curves have been displaced vertically for clarity.

structure characteristic, within the limits of the temperature dependence of the resolution. The above effects indicate that our structure is in no way related to thermally induced currents.

(3) Small (up to 100 Oe) dc magnetic fields have been applied in a direction parallel to the plane of the junction. The structure remains substantially unchanged over this range of field, as shown in Fig. 11. Occasionally, however, one or more of the narrower minima will be strongly affected as the field is varied, the amplitude of the  $dV/dI$  minimum being approximately periodic in applied field.

## B. Results

We have concluded that this fine structure is another example of the SHS in the Pb-I-Pb system, and have accordingly analyzed our data in terms of superposed subharmonic series. These series have the generic form  $V = V_c/m$ , where  $V_c$ , the leading term of the series, is approximately equal to  $2\Delta_{Pb}/e$ . The  $V_c$ , and the resulting fine structure, are assumed to arise from the effects of the energy-gap anisotropy in the superconducting Pb films. As previously mentioned, we have only been able to construct junctions whose constituent Pb films are both thicker than the coherence length. From an empirical standpoint, we are thus able to postulate only that  $eV_c = \Delta_{1c} + \Delta_{2c}$ , where  $\Delta_{1c}$  and  $\Delta_{2c}$  represent some critical value of the energy gap in films 1 and 2.

We have been able to analyze completely the fine SHS of our samples in terms of such  $V_c/m$  series, using a number of different values of  $V_c$  for each junction. As many as seven different  $V_c$  were necessary on a single junction in order to fit all the observed structure. Figure 12 illustrates how such a series may be fitted to our data. Table III summarizes the  $V_c$  values we have derived for several of these samples.

This fine SHS has been found to be similar in detail from junction to junction, particularly for junctions which have been deposited simultaneously on a single substrate. In the course of a given experiment at low temperature, the SHS of any junction was completely reproducible, and was found to be almost exactly symmetric about  $V=0$ . This reproducibility is maintained even if the junction is cycled repeatedly between 4.2°K and 1.2°K during the run. A more stringent test of reproducibility was performed by allowing one of the samples to warm very slowly to room temperature and, after a week's storage, cooling it gently back to liquid-He temperature. The  $dV/dI$  characteristic remained substantially unchanged by this cycling, the major effect being a slight loss of fine detail in some of the lower voltage structure.

Several attempts were made to induce strain in these samples by rapid thermal cycling, as we had done for Pb-I-Al junctions. Pb-I-Pb junctions treated in this manner were, however, invariably damaged irreparably by this treatment, usually by developing superconducting shorts across the junction.

The observations of Marcus<sup>61</sup> are pertinent here, as he used crossed Pb films approximately 1000 Å in thickness, so that  $d \approx \xi_0$ . Although his equipment was capable of resolving fine SHS had any been present, no such structure was observed. For the most part his curves display only the broad structure previously discussed, which is present even in the "dirty" film limit.

It has been suggested<sup>61</sup> that the SHS is a consequence of the presence of filamentary metallic shorts through the oxide layer, which are forced from the superconducting to the normal state by the excess current. The experience of this author, among others, is that junctions with such shorts show properties which are *not* observed in our data. Among the most noticeable of the shorting effects is the strong asymmetry of structure due to such effects about  $V=0$ . In addition, there is usually a great deal of hysteresis in the critical current of such shorts, so that there is a large difference between traces taken for increasing dc-current amplitude and those taken for decreasing amplitude. As our SHS exhibits neither of these properties, we believe we are justified in suggesting that our structure arises from a true tunneling process. We would also not expect to find the reproducibility of detail from junction to junction which our SHS exhibits unless such a tunneling process were involved.

Every one of our junctions which exhibited SHS also exhibited several phenomena arising from the Josephson effect. Among the experimental observations relating to this effect are:

(1) We observe a dc current at  $V=0$  which falls off rapidly if we apply a small magnetic field parallel to the junction. This current is observed to be periodic in field, with a period of the order of several Oe. Figure 13 shows the effect of magnetic field on this  $V=0$  cur-

rent for one of our samples. The reduction by a factor  $>10$  for an applied field of 6 Oe tends to indicate a "good" Josephson junction,<sup>64</sup> as opposed to a "supershorted" junction implied by a small field periodicity.

(2) The standing-wave modes<sup>65</sup> due to cavity resonances of the ac Josephson effect in the superconducting cavity formed by the two films are observed, as is also shown in Fig. 13. In order to observe the SHS at small biases, it was usually necessary to apply parallel magnetic fields of sufficient strength to suppress these standing-wave modes. We believe that the occasionally-seen magnetic field dependence of some of our lower voltage SHS peaks is due to their being superimposed on one of these cavity modes.

(3) Figure 13 also shows the structure in the  $I$ - $V$  curve which arises from the traveling-wave mode<sup>66</sup> of the ac Josephson effect in small magnetic fields. This effect is completely suppressed at the magnetic field strengths at which most of our data were taken.

These last two phenomena, which are manifestations of the ac Josephson effect, are both dependent on the presence of a reasonably high quality dielectric layer between the superconducting films. It is our contention that the presence of metallic shorts, whether superconducting or normal, connecting the two films would spoil the  $Q$  of the cavity to the extent that such phenomena could not be observed.

The present status of the theory of the SHS as a true tunneling process will be discussed in the next section. Despite the recent theoretical developments, no line-shape calculation can as yet be made. For this reason we remain unable to analyze our  $V_c$  values by any method analogous to the analysis used to identify the  $2\Delta_c$  values of the Pb- $I$ -Al junctions.

## VI. DISCUSSION

### A. Identification of Critical Values

The lack of theoretical comparisons for the SHS line shapes prevents us from either separating  $V_c$  values which  $=2\Delta_c$  from those which  $=\Delta_{1c}+\Delta_{2c}$ , or identifying the type of critical value involved. Nevertheless, a great deal of analysis of the data can be performed by comparing the SHS results for  $V_c$  with our  $2\Delta_c$  values obtained from the analysis of the Pb- $I$ -Al junctions. Table IV contains a summary of all the experimental data presented in this work, comparing the structure observed in the ordinary tunneling characteristic with the SHS.

From this comparison it has been possible to identify the  $V_c$  series at 2.44, 2.52, and 2.97 meV as being  $2\Delta_c$  series; the type of critical value involved has been determined from the Pb- $I$ -Al line shapes and has also been indicated in Table IV. As may be seen by a small

TABLE IV. Summary of experimentally determined values of  $V_c$  and  $2\Delta_c$  for Pb, extrapolated to  $T=0^\circ\text{K}$ .<sup>a</sup>

Type of critical value	$\langle V_c \rangle_{av}^b$ (meV)	$\langle 2\Delta_c \rangle_{av}^c$ (meV)	$k_B T_c$ (bulk) <sup>d</sup> units	$\text{cm}^{-1}$
...	$2.11 \pm 0.02$	...	3.40	17.0
...	$2.23 \pm 0.02$	...	3.60	18.0
...	$2.33 \pm 0.02$	...	3.76	18.8
...	$2.39 \pm 0.02$	...	3.85	19.3
Saddle point	$2.44 \pm 0.02$	$2.44 \pm 0.02$	3.93	19.7
Saddle point	$2.52 \pm 0.02$	$2.55 \pm 0.02$	4.11	20.5
...	$2.61 \pm 0.02$	...	4.21	21.0
Maximum	$2.97 \pm 0.02$	$2.99 \pm 0.02$	4.81	24.0

<sup>a</sup> The "average" gap of 2.71–2.75 meV has been omitted here.

<sup>b</sup> From Table III.

<sup>c</sup> From Table II.

<sup>d</sup>  $T_c(\text{bulk}) = 7.198^\circ\text{K}$ .

amount of manipulation of the given  $V_c$  values, it is quite possible that some of the  $V_c$  are, in fact, averages of two of the others.<sup>67</sup> For this reason we do not, despite the absence of  $V_c$  values between some of the known  $2\Delta_c$  values (2.44 and 2.55 meV for instance), feel justified in making the tempting assumption that all of the  $V_c$  values are actually  $2\Delta_c$ . We do, however, feel that the 2.97-meV value does represent the absolute maximum of the Pb energy gap, as no sign of any structure at larger gap values has been observed on any of our samples. As we have observed no minima on the Pb- $I$ -Al junctions, no similar statement can be made about the low-energy end of the gap spectrum, except to remark that no structure has as yet been observed which is attributable to a value of  $V_c$  smaller than 2.11 meV.

Most interesting is the absence of SHS from  $2\Delta = 2.71 - 2.75$  meV, a value which has long been identified as "the" double gap of Pb. Structure due to this gap is certainly the most prominent feature of the ordinary part of the tunneling characteristic in all of our tunneling junctions. Because of the lack of fine SHS from this value of the double gap, however, we maintain that this is not a critical value, but rather the average value of the Pb double gap over the energy-gap surface. As most of this surface consists of regions which are not in the vicinity of a critical value, most of the tunneling current will be connected with these nonsingular regions whose average double-gap value will lie, as stated, near 2.71–2.75 meV.

This would account for the prominence of this feature in the ordinary tunneling characteristic, particularly for the Pb- $I$ -Pb junctions, which exhibit no other structure at  $eV \approx 2\Delta$ . In the case of the SHS such an average value will be absorbed into the broad SHS rather than appear in the fine structure we have analyzed.

### B. Comparison with Theory

There are some discrepancies between the results shown in Table IV and Bennett's<sup>4</sup> theoretical predic-

<sup>64</sup> P. W. Anderson and J. M. Rowell, Phys. Rev. Letters **10**, 230 (1963); J. M. Rowell, *ibid.* **11**, 200 (1963).

<sup>65</sup> D. D. Coon and M. D. Fiske, Phys. Rev. **138**, A744 (1965).

<sup>66</sup> R. E. Eck, D. J. Scalapino, and B. N. Taylor, Phys. Rev. Letters **13**, 15 (1964).

<sup>67</sup> That is, if one  $V_c$  corresponds to  $2\Delta_{c1} = E_1$  and another  $V_c$  to  $2\Delta_{c2} = E_2$ , a third  $V_c$  halfway between the previous two may be either  $\Delta_{c1} + \Delta_{c2} = (E_1 + E_2)/2$  or  $2\Delta_{c3} = E_3$ .

tions of the anisotropic energy-gap surface of Pb. The more trivial of these discrepancies concerns the number of observed critical values. Assuming all our  $V_c$  to be  $2\Delta_c$  would raise the total number of experimentally observed critical values to eight. This compares with the theory, which predicts a total number of twelve critical values; four minima, five saddle points, and three maxima. The fact that not all of these are observed is, nevertheless, not altogether unexpected.

The most probable explanation of our having observed a smaller number of critical values than predicted is that some of these are almost degenerate in energy. If two critical values are within, say,  $10 \mu\text{eV}$  of each other, we would not be able to resolve them experimentally. This would certainly be the case if one of the degenerate critical values was a saddle point, with a strong experimental singularity, while the other was a less singular minimum or maximum. Such an occurrence is possible, since we are speaking only of *local* minima or maxima, and a saddle point on one part of the gap surface may have a lower (higher) energy than a minimum (maximum) on another part of the surface.

Secondly, we cannot rule out the possibility that the samples are to some degree oriented preferentially on the substrate. If such were the case we would see only those critical values which lie on portions of the surface where the electron group velocity is nearly normal to the plane of the junction.<sup>52</sup> A third possibility arises from the lack of any observed  $V_c$  values in the region of the average double gap. There may be a number of critical values in this region, lying close together in such a manner as to smear their structure into one rather broad peak which would not be sufficiently resolved to be experimentally identifiable.

Difficulties also arise when an attempt is made to make a quantitative comparison between the  $V_c$  values and the range of theoretically predicted critical values. Bennett has indicated that the range of the double gap on the Pb surface is from an absolute minimum of 2.55 meV to an absolute maximum of 2.86 meV, as opposed to the experimentally determined spread of 2.11 to 2.97 meV. The disparity is particularly severe at the low-energy end of the spectrum. Bennett has indicated that, under the assumptions of the theory, the total error in the calculation of the *anisotropic part* of the gap is less than 30% of its value. Assuming this maximum error would still leave the predicted spread of values short of the experimentally observed range. It must be noted, however, that raising the average double-gap value from the 2.70 meV used by Bennett to the 2.75 meV observed on our junctions, in conjunction with a 30% increase in the anisotropic part of the gap, would place the estimated maximum gap at 2.96 meV, very close to the observed value.

We believe that the discrepancy between the observed and predicted values of the range may be due to the use of an averaged, isotropic, electron-phonon coupling in the electron-phonon interaction. The in-

clusion of properly anisotropic coupling would be expected to increase the predicted anisotropy, perhaps sufficiently so as to obtain far better agreement with experiment. There would, however, appear to be no way at present to include such an anisotropic coupling without greatly increasing the difficulty of solving the gap equations.

### C. Comparison with Other Experiments

There have been a relatively small number of experimental observations of the energy-gap anisotropy of Pb. This is primarily a consequence of the difficulties<sup>68,69</sup> of applying to Pb the technique of acoustic attenuation, which has proved so fruitful in the case of other superconductors. Of the two remaining experimental methods for the investigation of anisotropy, one is tunneling, and the other far-infrared absorption,<sup>14</sup> which is one of the most difficult of experiments to perform with the necessary resolution. Although some structure in the far-infrared absorption edge has been reported<sup>70</sup> in the range of our critical values, such data as is available is of a preliminary nature, and we must await the appearance of more data before comparisons can be accurately made. We do note, however, that the smallest of our critical gap values does lie at an energy above that of the precursor absorption,<sup>71</sup> and cannot serve to explain the precursor.

Other tunneling experiments have indicated the presence of anisotropy in junctions of various compositions. In particular, Townsend and Sutton<sup>19</sup> have observed the presence of two Pb energy gaps in the characteristics of Pb-I-Ta tunneling junctions, at voltages corresponding to double-gap values of  $2.67 \pm 0.05$  meV and  $2.90 \pm 0.05$  meV. This is in good agreement with our observations.

It is to be hoped that more investigations of this phenomenon will be forthcoming, particularly by methods which measure  $2\Delta$  values only, so that a more detailed comparison with our results may be made.

### D. Possible Mechanisms for the SHS

#### *Multiparticle Tunneling*

The sharp excess-current step observed<sup>58</sup> at  $eV = 2\Delta/2$  has been treated theoretically by Schrieffer and Wilkins.<sup>72</sup> They attributed this effect to the simultaneous tunneling of two quasiparticles. This process is second-order in the tunneling Hamiltonian, and therefore the current varies as  $|T|^4$ . They were able to fit the data very well with this mechanism by invoking thin patches in the oxide layer. There is a very strong

<sup>68</sup> R. E. Love and R. W. Shaw, Rev. Mod. Phys. **36**, 260 (1964).

<sup>69</sup> B. R. Tittman and H. E. Bömmel, Phys. Rev. Letters **14**, 296 (1965).

<sup>70</sup> S. L. Norman and D. H. Douglass, Jr., Bull. Am. Phys. Soc. **11**, 87 (1966).

<sup>71</sup> P. L. Richards and M. Tinkham, Phys. Rev. **119**, 575 (1960).

<sup>72</sup> J. R. Schrieffer and J. W. Wilkins, Phys. Rev. Letters **10**, 17 (1963).

reason for postulating a different mechanism, however, in the case of our SHS. If we attempt to extend the two-particle tunneling to higher order subharmonics, we are forced to construct a multiparticle tunneling process, in which the current at a subharmonic step  $eV=2\Delta/m$  arising from the tunneling of  $m$  particles will be given by  $m$ th-order perturbation theory. In this case  $I \propto |T|^{2m}$ . The rapid fall-off of the  $|T|^{2m}$  term for increasing  $m$ , however, leads to predicted tunneling amplitudes for the SHS which are far too small to explain the observed effects.<sup>73</sup>

The fact that all of our Pb-I-Pb junctions which have SHS exhibit Josephson-effect phenomena has led us to believe that there is, however, a connection between our SHS and the ac Josephson effect.

#### The Josephson Effect

Josephson's solution to the problem of tunneling between two superconductors<sup>43</sup> may be expressed by the equation he has derived for the tunneling current. To first order,<sup>47</sup> this current is given by

$$I_{SS} = I_{SS}^0 + J_{SS} \sin \Phi, \quad (6.1)$$

where  $I_{SS}^0$  is the usual single-particle tunneling current given by Eq. (4.3). The  $J_{SS} \sin \Phi$  term represents the tunneling of *Cooper pairs*, and is the term neglected in the CFP treatment. For finite dc biases, the relationship between the phase and the bias is given by

$$\frac{\partial \Phi}{\partial t} = \frac{2eV}{\hbar}. \quad (6.2)$$

Equation (6.2), combined with Eq. (6.1), predicts an ac current through the barrier at finite biases, at a frequency of 483.6 MHz/ $\mu$ V. Recently a finite amount of radiated power has been extracted from such junctions,<sup>74,75</sup> confirming the reality of the ac current and verifying the frequency-voltage relationship.

The existence of this ac current suggests possible mechanisms for the SHS. The high power density of ac in the junction allows us to treat the barrier as a region containing a high density of photons. Owing to the nonlinear nature of the junction characteristic, there will be a very high harmonic content to the ac fields.

<sup>73</sup> For a typical tunneling junction, the factor  $e^{-\epsilon}$  appearing in the expression for  $|T|^2$  may be approximated, using the relation  $2(2m)^{1/2}/\hbar = 1.025 \text{ eV}^{-1/2} \text{ \AA}^{-1}$ , by  $\exp(-1.025 \langle \varphi \rangle_{av} d)$ , where  $\langle \varphi \rangle_{av}$  is a constant barrier potential, specified in electron volts, and  $d$  is the barrier thickness in  $\text{\AA}$ . Taking the parameters for a low-resistance junction, we may use  $\langle \varphi \rangle_{av} \approx 1 \text{ eV}$ ,  $d \approx 10 \text{ \AA}$ . In this case  $|T|^2 \approx 10^{-4}$ . Applying  $I \propto |T|^{2m}$  to the step at  $m=7$ , for instance, would then lead to the predicted multiparticle current being down by a factor of  $10^{-24}$  from the value of the  $m=2$  step. For these reasons we believe that our SHS is not due to multiparticle tunneling, a conclusion supported by our experimental observations, as mentioned previously.

<sup>74</sup> I. K. Yanson, V. M. Svistunov, and I. M. Dmitrenko, Zh. Eksperim. i Teor. Fiz 48, 976 (1965) [English transl.: Soviet Phys.—JETP 23, 650 (1965)].

<sup>75</sup> D. N. Langenberg, D. J. Scalapino, B. N. Taylor, and R. E. Eck, Phys. Rev. Letters 15, 294 (1965).

This is equivalent to stating that the barrier contains large numbers of harmonic photons whose frequencies are given by

$$\omega = \frac{2neV}{\hbar}, \quad (6.3)$$

where  $n$  is an integer. The absorption of such a photon by a single particle will allow the particle to tunnel whenever its energy plus the photon energy equals  $2\Delta$  (in the identical superconductor case). Therefore, a current threshold is expected to occur whenever  $eV=2\Delta/(1+2n)$ . This yields a subharmonic series for odd  $m$  values. A similar series for even  $m$ , however, is more difficult to construct on this elementary model.

Werthamer<sup>76</sup> has performed a calculation of the "strongly self-coupled" Josephson junction in which he treats the junction as an oscillator with strong self-coupled feedback. He has pointed out that there is a possible subharmonic series arising from the pair-tunneling singularity first pointed out by Riedel,<sup>77</sup> who calculated the amplitude of the ac pair tunneling current using the Green's function formalism of Ambegaokar and Baratoff,<sup>47</sup> and discovered that, for the two-identical-superconductor case, the ac pair current exhibits a logarithmic singularity at  $eV=2\Delta$ .

In treating pair processes, we recall that the chemical potential is the energy *per particle*, and thus the energy of a pair is twice the chemical potential. The change in energy for a pair tunneling across a barrier biased at  $eV$  is, therefore, given by  $\delta E=2eV$ . Restricting ourselves once again to the case of two identical superconductors, the energetics of the Riedel mechanism are such that the singularity occurs whenever the energy difference  $\delta E$  of the pairs across the barrier is given by  $\delta E=2eV=4\Delta$ , which occurs at a dc bias of  $V=2\Delta/e$ . In the case of the strongly self-coupled junction, a Riedel-type singularity in the current will occur whenever the dc bias satisfies the relation

$$eV = \frac{2\Delta}{1+2n}, \quad (6.4)$$

which gives an odd subharmonic series.<sup>78</sup> Due to the increasing power being put into the ac field at these Riedel singularities, there will be a dc peak in the tunneling current at biases corresponding to the ac current peaks. The shape of the former will depend on the strength of the junction self-coupling as well as on the actual shape of the Riedel singularity, which is expected

<sup>76</sup> N. R. Werthamer, Phys. Rev. 147, 255 (1966).

<sup>77</sup> E. Riedel, Z. Naturforsch. 19a, 1634 (1964).

<sup>78</sup> The reason for having an odd series rather than a complete series is as follows: Josephson tunneling takes place via a virtual intermediate state in which a pair is broken and one partner transferred across the barrier. The Riedel-Werthamer calculation shows that there is a minimum energy denominator ( $2\Delta - eV - \hbar\omega$ ) associated with this intermediate single-particle state. Using Eq. (6.3), this produces a logarithmic singularity in the sum over the intermediate states whenever Eq. (6.5) is satisfied.

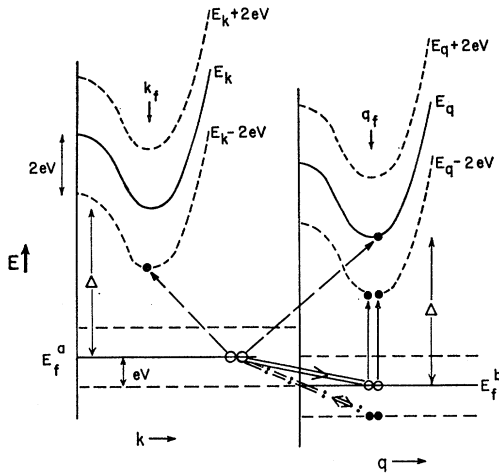


FIG. 14. Schematic diagram of the three SHS mechanisms, shown with a common initial state. The excited levels of the quasi-particle distribution occur at  $\pm 2neV$  from the unperturbed levels  $E_k$  and  $E_q$ . Since the energy of a pair must be divided by two to be plotted on a single-particle diagram of this type, the excited pair levels are located at  $\pm neV$  from the Fermi energies. Final states are shown as solid dots. The probability for a Cooper pair to tunnel varies as  $|T|^2$ , as it does for a single particle.

to be rounded off by finite temperature and lifetime effects.

There will also be steps in the current arising from single-particle photon-assisted tunneling processes. The odd terms in this series arise from the Dayem-Martin-Tien-Gordon<sup>79,80</sup> type of effect proposed earlier, in which a single particle tunnels by absorbing a Josephson photon. This will give current *steps* at biases given by  $eV = 2\Delta/(1+2n)$  (for the two-identical-superconductor case) so that the  $m$ th subharmonic step is caused by the  $\frac{1}{2}(m-1)$ th harmonic of the ac Josephson frequency. The even series terms arise from the tunneling of a Cooper pair, which is broken up into two single-particle excitations *after* it has tunneled, or the mirror mechanism consisting of the excitation of two single particles followed by the tunneling of a Cooper pair. In both of the even cases the coupling of the pair to the excitations is through the radiation field, and the prediction of this particular even series is unique to Werthamer's results. In either case, a photon may be absorbed to conserve energy, and the result will be a series of current steps at biases given by  $eV = 2\Delta/2n$ , so that the  $m$ th subharmonic step arises from the  $\frac{1}{2}m$ th harmonic of the ac Josephson frequency.

These three processes are schematically indicated in Fig. 14, which represents tunneling between two identical superconductors in the electron-excitation representation proposed by Schrieffer.<sup>81</sup> In this representation, the  $E$ -versus- $k$  spectrum for quasielectrons only is drawn, with all values of  $k$  available for excitations

above the Fermi energy. The Fermi level  $k_f$  is located at the minimum of the excitation spectrum, i.e. at  $E = \Delta$ . At  $T = 0^\circ\text{K}$  all electrons are condensed into Cooper pairs, which are localized at the Fermi energy, so that such a pair is the only viable initial state. The modulation of the pair levels at  $\pm neV$  about the Fermi surface, and of the single particle spectrum at  $\pm 2neV$  about the unmodulated spectrum, is indicated by dotted lines. For the sake of clarity, only the  $n=1$  levels are shown. In terms of the energy requirements, as only photon absorption is to be considered, levels below the unmodulated level are available only for final states, and levels above only for initial states. The even single-particle series (single-particle in the sense that the final state consists of two single-particle excitations) is indicated in solid lines. The odd single-particle series is indicated in long dashes, and corresponds closely to the Dayem-Martin-Tien-Gordon effect which is obtained by external modulation of the junction. The Riedel-Werthamer term is indicated by a dash-dot pattern, and corresponds to straightforward ac pair tunneling, as indicated by the two-way arrows. As mentioned, only the  $n=1$  mechanisms are indicated here, although the junction is drawn, for clarity, at a much lower bias than the threshold at which the indicated processes occur. In terms of subharmonic number, these processes correspond to an  $m=3$  Riedel-Werthamer peak, an  $m=3$  odd-series step, and an  $m=2$  even-series step.

It is most important to note that the three contributions to the SHS described above are all first order in the tunneling Hamiltonian, going as  $|T|^2$  for all subharmonics, and thus are in closer agreement with the inferences drawn from the experimental data than previous theories of higher order in the perturbation. Unfortunately, it has not been possible to compare our line shapes with theoretical estimates, as we are unable to estimate either the strength of the coupling in the junctions measured, or the effects of finite temperature on the theoretical predictions. We also remark that thus far all of our data appears to be composed of steps rather than peaks on the  $I$ - $V$  characteristic. Additionally, we have seen SHS at biases lying between the standing-wave cavity modes, which would seem to violate the basic assumption of the theory. In the absence of information regarding the various parameters involved, however, we can make no definitive statement regarding the difficulties presently encountered in attempting to relate the theory to the experimental data.

#### ACKNOWLEDGMENTS

The author wishes to express his thanks to Dr. A. J. Bennett for many long and fruitful discussions concerning the theory of the anisotropy, Dr. M. H. Cohen and Dr. L. M. Falicov for many interesting and informative discussions, Dr. R. W. Johnson for advice in setting up the high-vacuum system, and Dr. N. R.

<sup>79</sup> A. H. Dayem and R. J. Martin, Phys. Rev. Letters **8**, 246 (1962).

<sup>80</sup> P. K. Tien and J. P. Gordon, Phys. Rev. **129**, 647 (1963).

<sup>81</sup> J. R. Schrieffer, *Theory of Superconductivity* (W. A. Benjamin, Inc., New York, 1964).

Werthamer for a discussion of his results prior to publication. I am particularly indebted to Dr. D. H. Douglass, Jr., who first suggested this problem, and whose advice and guidance throughout this work have been of inestimable value.

The research was supported in part by the Army Research Office (Durham) and the Advanced Research Projects Agency. The use of the facilities of, and the technical assistance of the personnel of, the Low Temperature Laboratory, supported by the National Science Foundation, and the Materials Preparation Laboratory, supported by the Advanced Research Project Agency, are gratefully acknowledged.

### APPENDIX A

To illustrate the effect gap anisotropy may have on  $\rho(E)$ , let us consider a model distribution function<sup>82</sup>

$$\begin{aligned} g(x) &= A(x - \Delta_m), & \Delta_m \leq x \leq \Delta_{av} \\ &= A(\Delta_M - x), & \Delta_{av} \leq x \leq \Delta_M \\ &= 0 & \text{elsewhere,} \end{aligned} \quad (\text{A1})$$

where  $\Delta_m$  is the minimum value of the energy gap,  $\Delta_M$  is the maximum value, and  $\Delta_{av}$  is the average value of the gap,  $\Delta_{av} = (\Delta_m + \Delta_M)/2$ . For our model calculation we set  $\Delta_m = 1.20$  meV,  $\Delta_M = 1.50$  meV and  $\Delta_{av} = 1.35$  meV; these are reasonable values for the range and average value of the energy gap of superconducting Pb. Performing the integration of Eq. (4.6) we find

$$\rho(E) = EA \left\{ (E^2 - \Delta_m^2)^{1/2} + \Delta_m \left[ \sin^{-1} \left( \frac{\Delta_m}{E} \right) - \frac{\pi}{2} \right] \right\} \quad (\text{A2})$$

for  $\Delta_m \leq E \leq \Delta_{av}$ ,

$$\begin{aligned} \rho(E) = EA \left\{ (E^2 - \Delta_m^2)^{1/2} - 2(E^2 - \Delta_{av}^2)^{1/2} \right. \\ \left. - \Delta_M \left[ \sin^{-1} \left( \frac{\Delta_{av}}{E} \right) - \frac{\pi}{2} \right] \right. \\ \left. + \Delta_m \left[ \sin^{-1} \left( \frac{\Delta_m}{E} \right) - \sin^{-1} \left( \frac{\Delta_{av}}{E} \right) \right] \right\} \quad (\text{A3}) \end{aligned}$$

for  $\Delta_{av} \leq E \leq \Delta_M$ , and

$$\begin{aligned} \rho(E) = EA \left\{ (E^2 - \Delta_m^2)^{1/2} + (E^2 - \Delta_M^2)^{1/2} \right. \\ \left. - 2(E^2 - \Delta_{av}^2)^{1/2} + \Delta_M \left[ \sin^{-1} \left( \frac{\Delta_M}{E} \right) - \sin^{-1} \left( \frac{\Delta_{av}}{E} \right) \right] \right. \\ \left. + \Delta_m \left[ \sin^{-1} \left( \frac{\Delta_m}{E} \right) - \sin^{-1} \left( \frac{\Delta_{av}}{E} \right) \right] \right\} \quad (\text{A4}) \end{aligned}$$

<sup>82</sup> We have deliberately chosen a distribution which goes smoothly to zero at both limits to avoid the introduction of spurious singularities into  $\rho(E)$ . The sharp break in  $\rho(E)$  in the model calculation of Ref. 4 is a consequence of the use of a rectangular model, which does not meet the above requirement.

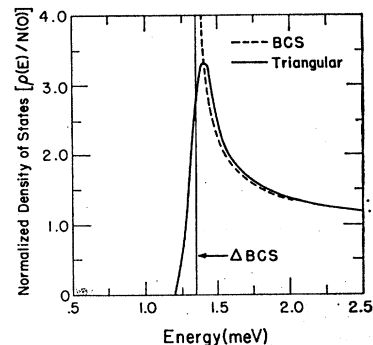


FIG. 15. The density of states for a model anisotropic superconductor with a triangular gap distribution, compared to the isotropic (BCS) density of states.

for  $E > \Delta_M$ . This solution is shown in Fig. 15, together with the BCS expression of Eq. (4.8), with  $\Delta_{BCS}$  set at  $1.35$  meV  $= \Delta_{av}$ . Both solutions are normalized so that  $\rho(E) \rightarrow N(0)$  in the limit  $E \rightarrow \infty$ . It is clearly seen that the general effect of the anisotropy is to round off the singularity which is present in the isotropic form of  $\rho(E)$ .

### APPENDIX B

Let us consider as an example the case of an isotropic-superconductor (1)-anisotropic-superconductor (2) junction in the neighborhood of  $eV = \Delta_1 + \Delta_{2sp}$  at  $T = 0^\circ\text{K}$ . Using Table I, together with Eqs. (4.6) and (4.9), we obtain, for  $eV < \Delta_1 + \Delta_{2sp}$ ,

$$I_{<} \propto \int_{-Q}^{-\Delta_1} dE \frac{E}{(E^2 - \Delta_1^2)^{1/2}} (\Delta_{2sp} - E - eV)^{1/2}, \quad (\text{B1})$$

where the lower limit  $Q$  has no significant effect on the calculation in the region of interest. Taking  $Q$  to be close to  $\Delta_1$ , we may approximate (B.1) by

$$I_{<} \approx P' \int_{-Q}^{-\Delta_1} dE \left( \frac{\Delta_{2sp} - E - eV}{E + \Delta_1} \right)^{1/2}, \quad (\text{B2})$$

where  $P'$  is approximately constant over the region of integration. This may be integrated easily to yield

$$I_{<} \approx \alpha + \beta(\Delta_1 + \Delta_{2sp} - eV), \quad (\text{B3})$$

where  $\alpha$  and  $\beta$  are constants, so that

$$(dI/dV)_{<} = \text{const.} \quad (\text{B4})$$

(We calculate here  $dI/dV$  and  $d^2I/dV^2$ , since they are directly obtainable from the tunneling integral. To convert, one merely needs use the relations  $dV/dI = (dI/dV)^{-1}$  and  $d^2V/dI^2 = (dI/dV)^{-3}(d^2I/dV^2)$  to obtain the values given in the text.)

Making the same approximations again, we obtain for  $eV > \Delta_1 + \Delta_{2sp}$

$$\begin{aligned} I_{>} \approx P' \int_{-Q}^{-eV + \Delta_{2sp}} dE \left( \frac{\Delta_{2sp} - E - eV}{E + \Delta_1} \right)^{1/2} \\ + P'' \int_{-eV + \Delta_{2sp}}^{-\Delta_1} \frac{dE}{(E + \Delta_1)^{1/2}}, \quad (\text{B5}) \end{aligned}$$

where  $P'$  and  $P''$  are both constant over the regions of integration. Performing the integration we obtain

$$I_{>} \approx \alpha' (\Delta_{2sp} + \Delta_1 - eV)^{1/2}, \quad (\text{B6})$$

and therefore<sup>83</sup>

$$(dI/dV)_{>} \propto (\Delta_{2sp} + \Delta_1 - eV)^{-1/2}. \quad (\text{B7})$$

Let us now consider a junction composed of two identical anisotropic superconductors at  $T=0^\circ\text{K}$ . Since the most singular behavior will occur near a saddle point (cf. Fig. 6 and Table I) we consider the case of  $eV \sim 2\Delta_{sp}$ . For  $eV < 2\Delta_{sp}$ ,

$$\begin{aligned} I_{<} \approx & P' \int_{-Q}^{-\Delta_{sp}} E(\Delta_{sp} - E - eV)^{1/2} dE \\ & + P'' \int_{-\Delta_{sp}}^{-eV + \Delta_{sp}} (\Delta_{sp} + E)^{1/2} (\Delta_{sp} - E - eV)^{1/2} dE \\ & + P''' \int_{-eV + \Delta_{sp}}^{-Q'} (\Delta_{sp} + E)^{1/2} (E + eV) dE, \quad (\text{B8}) \end{aligned}$$

where again  $P'$ ,  $P''$ , and  $P'''$  are constant over the regions of integration, while  $Q$  and  $Q'$  do not affect the results in any significant manner. Performing the integration, and taking the derivative with respect to  $V$ , we obtain

$$(dI/dV)_{<} = \alpha + \beta(2\Delta_{sp} - eV)^{3/2} + \gamma(2\Delta_{sp} - eV)^{1/2}, \quad (\text{B9})$$

<sup>83</sup> Note that here  $d^2I/dV^2 \propto (\Delta_{2sp} + \Delta_1 - eV)^{-3/2}$ , so that  $d^2V/dI^2$ , which goes as  $-(dI/dV)^{-3}(d^2I/dV^2)$ , is nonsingular.

so that there is no singularity in the first derivative. There is however, a singularity in the second derivative

$$(d^2I/dV^2)_{<} \propto (2\Delta_{sp} - eV)^{-1/2}. \quad (\text{B10})$$

For  $eV > 2\Delta_{sp}$  we obtain, similarly,

$$\begin{aligned} I_{>} \approx & P' \int_{-Q}^{-eV + \Delta_{sp}} E(\Delta_{sp} - E - eV)^{1/2} dE \\ & + P'' \int_{-eV + \Delta_{sp}}^{-\Delta_{sp}} E(E + eV) dE \\ & + P''' \int_{-\Delta_{sp}}^{-Q'} (\Delta_{sp} + E)^{1/2} (E + eV) dE. \quad (\text{B11}) \end{aligned}$$

After integration with respect to  $E$  and differentiation with respect to  $V$  we obtain

$$(dI/dV)_{>} = \alpha + \zeta(2\Delta_{sp} - eV)^{3/2} + \eta(2\Delta_{sp} - eV)^{5/2}, \quad (\text{B12})$$

so that

$$(d^2I/dV^2)_{>} \approx \text{const}. \quad (\text{B13})$$

Therefore, for the anisotropic-anisotropic case we see that in the limit as  $eV \rightarrow 2\Delta_{sp}$

$$(dI/dV)_{2\Delta_{sp}} = \text{continuous} \quad (\text{B14})$$

and

$$(d^2I/dV^2)_{2\Delta_{sp}} \propto \begin{cases} (2\Delta_{sp} - eV)^{-1/2} & eV < 2\Delta_{sp} \\ \text{const} & eV > 2\Delta_{sp} \end{cases}. \quad (\text{B15})$$